# Towards Sustainable Oxalic Acid from $CO_2$ and Biomass

Eric Schuler,*[a] Marilena Demetriou,[a] N. Raveendran Shiju,[a] and Gert-Jan M. Gruter*[a, b]

To quickly and drastically reduce $CO_2$ emissions and meet our ambitions of a circular future, we need to develop carbon capture and storage (CCS) and carbon capture and utilization (CCU) to deal with the $CO_2$ that we produce. While we have many alternatives to replace fossil feedstocks for energy generation, for materials such as plastics we need carbon. The ultimate circular carbon feedstock would be $CO_2$. A promising route is the electrochemical reduction of $CO_2$ to formic acid derivatives that can subsequently be converted into oxalic acid. Oxalic acid is a potential new platform chemical for material production as useful monomers such as glycolic acid can be derived from it. This work is part of the European Horizon 2020 project "Ocean" in which all these steps are developed. This Review aims to highlight new developments in oxalic acid production processes with a focus on $CO_2$-based routes. All available processes are critically assessed and compared on criteria including overall process efficiency and triple bottom line sustainability.

## 1. Introduction

Climate change, plastic pollution, and the loss of biodiversity are highly debated all over the planet ranging from denial to calls for system change, a green new deal, or even rebellion.[1–4] Science shows that the global climate is changing and that anthropogenic greenhouse gas emissions, mainly $CO_2$, are largely to blame.[5] As shown in Figure 1, still billions of tons of $CO_2$ are dumped into the environment every year with the number on the rise. In 2019, 940 million tons more $CO_2$ was emitted compared to the 42.14 Gt emitted in 2018, because fossil feedstocks still primarily fuel our lifestyle and economy. Even the effects of the global pandemic could reduce the $CO_2$ emissions in 2020 only down to 2017 levels.[6,7]

Consequently, we need to turn the ship around quickly and drastically reduce emissions. One way to do this is through carbon capture and storage (CCS) and carbon capture and utilization (CCU).[9–12] While we have many non-carbon alternatives to replace fossil feedstocks for energy generation, for materials such as plastics we need carbon. Next to biomass and waste, $CO_2$ is the only other carbon feedstock we have available.[13] Using $CO_2$ as a feedstock will be a requirement for meeting our ambitions of a circular future and staying within the planetary boundaries.[10,11,14–16]

Today, the chemical industry is still a big $CO_2$ emitter and lacks circularity as fossil-based feedstocks dominate.[17] However, the industry can also make use of $CO_2$ as a feedstock and therefore will be a key player in the energy and material transition and has the potential to change from a non-circular $CO_2$-emitting industry to a circular industry providing a possible net carbon sink.[9,12,18–21]

$CO_2$ can replace fossil feedstock in certain chemical processes and has the added advantage of being a low-cost or (with taxes) a potential negative-cost carbon source.[22] Converting $CO_2$,however, is not easy due to its high thermodynamic stability.[23–25] To drive the conversions of $CO_2$ to valuable products it requires high temperatures in chemo catalytic processes or high cell potentials in electro catalytic processes.[29–31] Today there is serious interest in $CO_2$ conversion technologies, with research mainly focused on the first step, the $CO_2$ reduction.However, we also require fully integrated downstream processes for a successful implementation of $CO_2$ as a feedstock.[26,27] To create circular materials, systemic changes will be required not only in the used feedstock but also in the design of products.[19] Consequently, different or new chemical processes will be required for which a robust life-cycle assessment will result in a significantly improved carbon footprint.[9,13,27]

The electrochemical fixation of $CO_2$ as formate is an interesting first step for $CO_2$ utilization. A full process starting with $CO_2$ to formate was developed at Liquid Light, a spin-off of Princeton University, which received broad scientific, commercial, and public interest.[28,29] Liquid Light, now part of Avantium, has successfully developed the gas-diffusion electrode-driven formate production from $CO_2$.[30–32] These electrodes are technology leaders due to the stability, scale, and performance of this $CO_2$ conversion.[33] The formate produced in the electrochemical cells is further "upcycled" to oxalate using a process called formate coupling, where two formate molecules combine to oxalate with the release of hydrogen.[34,35] Finally oxalate is acidified (e.g., in a multi-compartment electrochemical ion exchange cell), resulting in oxalic acid. Today, this technology is further developed in the public-private European Committee-

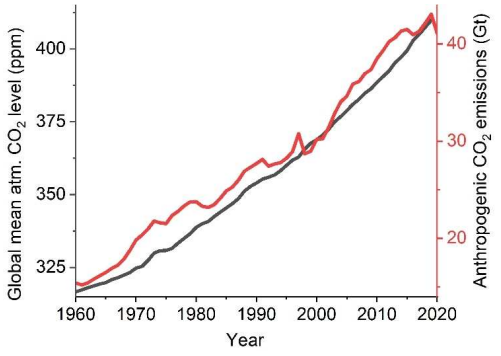


**Figure 1.** Annual $CO_2$ emissions caused by the release of fossil carbon and land-use change and development of global mean atmospheric $CO_2$ level.[6,7]

[a] E. Schuler, M. Demetriou, Dr. N. R. Shiju, Prof. G.-J. M. Gruter
Van 't Hoff Institute for Molecular Sciences
University of Amsterdam
Science Park 904, 1090 GD Amsterdam (The Netherlands)
E-mail: e.schuler@uva.nl
g.j.m.gruter@uva.nl
[b] Prof. G.-J. M. Gruter
Avantium Chemicals BV
Zekeringstraat 29, 1014 BV Amsterdam (The Netherlands)

sponsored partnership program OCEAN and implemented in different demonstration plants, which will be operational during 2021.[36] The business-case developed in this program suggests a production cost for formate of about €1000 $ton^{-1}$ at currently achieved process costs (Cell cost €5000 $m^{-2}$; current density 2000 $A\,m^{-2}$; faradaic yield $>90\%$), a $CO_2$ price of €50 $ton^{-1}$ for capture and purification and electricity prices of €30–50 $MWh^{-1}$. We project the production cost of formate to drop to €300–400 $ton^{-1}$ beyond 2030 with lower or negative $CO_2$ cost, a reduced electricity price, a reduction in cell cost, and improved current densities. This would make oxalic acid from formate an interesting competing feedstock for producing glycolic acid, glyoxylic acid, and even mono-ethylene glycol (MEG).

### 1.1. Oxalic acid and its valuable derivatives

Oxalic acid, the simplest of the dicarboxylic acids, is one of the oldest known acids, discovered by Scheele in 1734.[37] Today it is used in various industries. The largest consumer is the pharmaceutical industry, while others include agriculture, textiles and leather, and the chemical industries.[38–40] It is also widely used as an acid rinse in laundries, where it is effective in removing rust and ink stains as it converts most insoluble iron compounds into a soluble complex ion.[41] Similarly, oxalic acid is a well-known leaching agent for solubilizing heavy metals in bauxite, clay, and sewage sludge or bio-metallurgy for electronic waste.[42] As oxalic acid is naturally present in many vegetable food products it may also be used as a natural anti-browning and preservation agent in fruit and vegetable storage and can replace currently used inorganic acids.[43]

The oxalic acid market today is 350000 $t\,yr^{-1}$, but in the future, oxalic acid can be the origin of a wide range of high-value and high-volume chemicals. Two examples are formic acid/formate with a market of 900000 $t\,yr^{-1}$ or MEG with 30000000 $t\,yr^{-1}$. Of course, we can produce these chemicals from different resources, but if we want to avoid using fossil feedstock by 2050, the only alternative carbon sources are biomass and $CO_2$.[44,45] It has the potential to be a major platform for carbon-containing materials such as new classes of polymers.[46] This does not only include products derived directly from oxalic acid but also the oxalic acid-based $C_2$ compounds shown in Figure 2. We work on various processes to obtain these building blocks from oxalic acid and on several classes of oxalic acid- and glycolic acid-based polyesters.[36,46,47]

Glyoxylic acid is the first reduction product of oxalic acid. It is an important $C_2$ building block for many organic molecules of industrial importance, used in the production of agrochemicals, aromas, cosmetic ingredients, pharmaceutical intermediates, and polymers.[48–51] Glyoxylic acid finds direct application in personal care as neutralizing agent; it is widely used in hair straightening products in particular (shampoos, conditioners, lotions, creams) at levels of 0.5–10%.

If the aldehyde function of glyoxylic acid is further reduced, glycolic acid is obtained. Glycolic acid is a useful intermediate

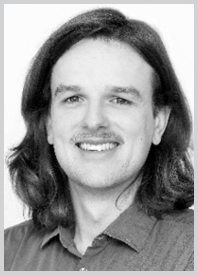

Eric Schuler is a Ph.D. candidate at the University of Amsterdam in the Catalysis Engineering group of Dr. Shiju Raveendran and Industrial Sustainable Chemistry group of Prof. Gruter. He obtained his Bachelor in Biochemistry with a specialization on proteomics at the Ruhr-University of Bochum. After a research stay at Macquarie University in Sydney, he obtained his Master in Chemistry from the University of Amsterdam with a specialization in sustainable chemistry and environmental studies. His research now focuses on the conversion of formate from $CO_2$ to monomers for polymers using catalysis and process optimization.

Shiju Raveendran is an Associate Professor at the University of Amsterdam and leads the Catalysis Engineering Group. He obtained his Ph.D. in Catalysis from the National Chemical Laboratory, Pune, India. After postdoctoral stays in UK and USA, he joined the University of Amsterdam as a faculty member in 2009. His research focuses on the engineering of heterogeneous catalysts in industrially important reactions including $CO_2$ conversion, biomass conversion, and lower alkane activation to chemicals and fuels.

Marilena Demetriou received her B.Sc. degree in Chemistry with a specialization in Material Chemistry from the University of Cyprus. Then, she moved to the Netherlands for a research traineeship in the University of Groningen where she worked in the field of homogeneous catalysis at Barta's group. Later, she received her M.Sc. in Chemistry from the University of Amsterdam/VU Amsterdam and did research at the HSCS group of UVA under the supervision of Dr. Shiju Raveendran. Her focus is on the synthesis of novel biobased monomers by heterogeneously catalyzed esterification.

Gert-Jan M. Gruter is CTO of technology company Avantium and Professor of Industrial Sustainable Chemistry at the University of Amsterdam. He has a background in polymer chemistry (DSM 1993–2000 and Eindhoven University of Technology 1999–2006). At Avantium he initiated the development for technologies to produce biobased polyesters. He is working on cascading of lignocellulosic biomass to produce 2G glucose as well as on the electrochemical reduction of $CO_2$ to formate and CO and downstream formate conversions to polyester monomers such as oxalic acid, glycolic acid, and subsequent polymers. At the University of Amsterdam he is working on novel sustainable plastics, plastic biodegradation, chemical recycling of polyesters, consumer psychology, and ocean plastics.

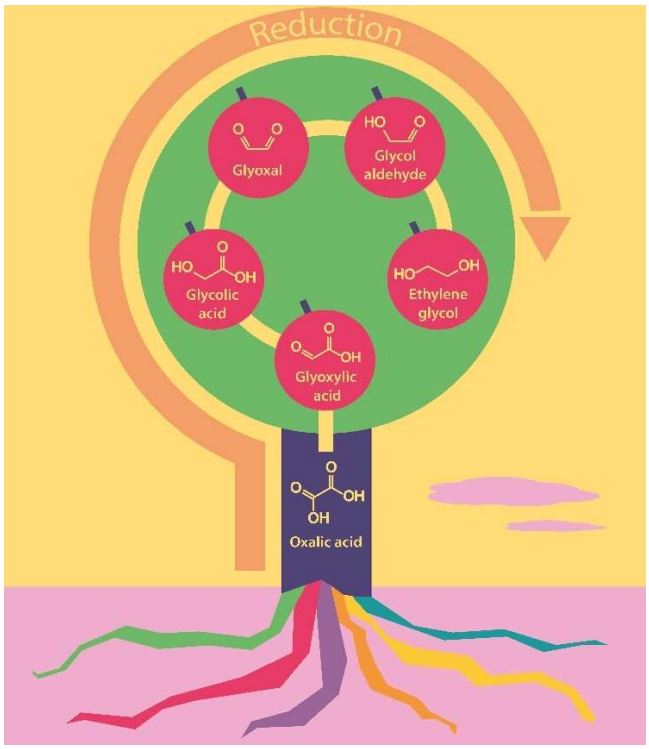


**Figure 2.** Value tree: Oxalic acid as starting compound for a variety of high-value products.

for organic synthesis, in a range of reactions including oxidation-reduction, esterification, and long-chain polymerization. It is used as a monomer in the preparation of polyglycolic acid and other biocompatible copolymers such as poly lactic-co-glycolic acid (PLGA.)[47,52] Glycolic acid is directly used in the textile industry as a dyeing and tanning agent, in food processing as a flavoring agent, and as a preservative. In the pharmaceutical industry, it is used as a skin care agent, and it is also used in adhesives and polymers.[53–55] Glycolic acid is often included in emulsion polymers, solvents, and additives for ink and paint to improve flow properties and impart gloss.[56]

From a commercial perspective, important derivatives of glycolic acid include the methyl and ethyl esters, which are readily distillable, unlike the parent acid. The butyl ester is a component of some varnishes, being desirable because it is nonvolatile and has good dissolving properties.

At the same reduction level is glyoxal. Due to its bifunctionality, it finds a wide range of applications. It is used as a cross-linker for condensation reactions with starch, cellulose, keratin, casein, animal glue, and mineral-based building materials. In organic synthesis, it is used to create heterocycles such as imidazole. In polymer chemistry, glyoxal is used as a solubilizing agent and cross-linking agent.[57] It is used directly in the cosmetic, textile, paper, and leather industry. In the oil industry, it is utilized as a sulfur-capturing agent.

Glycolaldehyde is the smallest sugar molecule and an interesting platform chemical itself.[58] It is used today in the polymer industry to create polymers with free hydroxy groups and in the production of furans.[59]

Lastly, there is MEG. One of the uses of ethylene glycol is as heating or cooling fluid with a broad range of applications. The largest use is in the polymer industry: ethylene glycol is an important monomer for polyethylene terephthalate (PET) polyester for fibers, bottles, and films. Because of its high boiling point and affinity for water, ethylene glycol is also a useful desiccant.

In addition to their current uses, all five $C_2$ compounds above are of increasing interest for the manufacture of new, high-performance polymers. Glyoxylic acid esters can be polymerized with bases to obtain biodegradable polymers with chelating properties.[60,61] Many monomers for sustainable polymers can be derived from it, linking the consumption of $CO_2$ with the production of circular, potential long-term carbon storage in materials.[62] A detailed account from our group on polyesters from oxalic acid and glycolic acid was published recently by Murcia Valderrama et al.[46]

These new solutions are required to satisfy the growing demand for polymers in the world with sustainable alternatives by replacing their petrochemical counterparts. The $CO_2$ volume potential in polymer applications will be very dependent on the economics of these monomers and the performance of the resulting polymer materials. In our group, we have shown very promising results towards meeting both these criteria.[63] Overall, we hope to show in this Review and in the years to come that oxalic acid has great potential the future because of its large potential applications in the polymer market.

In this Review, we discuss the popular pathway for $CO_2$ to oxalic acid developed by Liquid Light in detail and compare it to other production processes utilizing non-fossil carbon ($CO_2$ and biomass). We discuss each of the six main paths that we identified and highlight the upstream processes required for feedstock generation. To compare and assess the various possible pathways based on their sustainability and circularity, we use the concept of circular chemistry as a framework. This furthermore helps to identify optimization potential for resource efficiency across chemical value chains and enables a closed-loop, waste-free chemical industry, replacing today's linear "take-make-dispose" approach with circular processes.[19] Therefore, new processes should fit within the guiding principles of this framework.

## 2. Routes and Feedstocks to Oxalic Acid

Oxalic acid can be produced via six main routes as shown in Figure 3. The feedstocks, which include $CO_2$, CO, alkali formate (AF), ethylene glycol (EG), propylene, and carbohydrate-rich biomass, can be derived from three main sources: biomass, $CO_2$, and fossil carbon deposits. Some of these processes are commercially used whilst others are new developments. To improve their sustainability, we can either substitute fossil-based building blocks by renewable ones or develop new sustainable routes towards oxalic acid. Oxalic acid is commer-

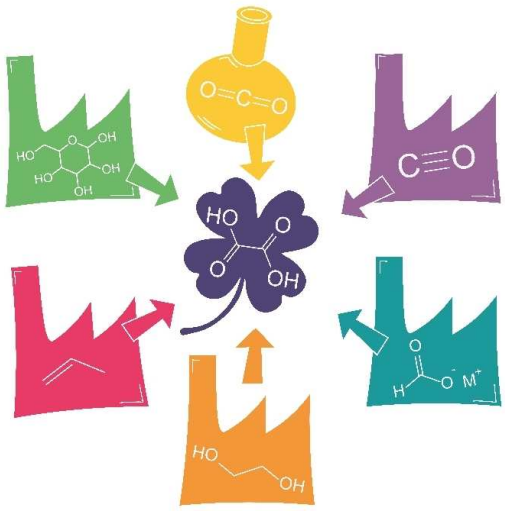

**Figure 3.** Overall there are six feedstocks directly used for oxalic acid-producing processes. These feedstocks include (1) $CO_2$, (2) CO, (3) alkali formate, (4) ethylene glycol, (5) propylene, and (6) carbohydrates. Except for $CO_2$, a commercially used route exists for all of those feedstocks.

cially produced today from carbohydrates, ethylene glycol, propylene, CO, and ethanol as well as alkali formates.

The oldest route towards oxalic acid was discovered by Bergmann in 1776. It requires the use of nitric acid to oxidize biomass, or more precisely the contained carbohydrates, into oxalic acid.[37] Biomass describes plant matter that originates from the photosynthetic conversion of $CO_2$ into sugars and other organic building blocks.[64] One of the main concerns for large-scale implementation of biomass as a feedstock for the chemical industry is its competition with food production when crops are used that are grown on farmland or are otherwise food themselves, such as corn or wheat.[65]

Although there is no competition with food today (due to the very small bio-based polymer volumes), it is important to develop so-called second- or third-generation biomass sources, which avoid this problem for future large-scale applications.[66] Scheme 1 shows all pathways that use biomass as feedstock. Besides nitric acid oxidation, biomass can be directly converted to oxalic acid by a process called alkali heating and fermentation.[43,67–100] Furthermore, biomass can also be used as a feedstock for the production of other oxalic acid precursors such as CO (gasification), $CO_2$ (fermentation or combustion), AF, and EG (via bio-ethylene or direct hydrogenolysis).[101,102]

Today the chemical sector is the largest industrial consumer of both oil and gas, accounting for 15% of oil and 9% of gas demand.[103] Together with coal, non-renewable fossil resources provide 87–96% of organic chemicals today, and oxalic acid is no exception.[103–105] Currently, the majority of oxalic acid is produced from fossil naphtha via propylene and ethylene glycol or CO, which is mainly obtained from coal.[106,107] Additionally, AF can be derived from fossil-based CO too.[108–114] Scheme 2 shows all fossil carbon-based pathways including oxidative pathways via naphtha-derived ethylene and propylene with harsh oxidants. This synthetic strategy was first reported by Gallently in 1881, who formed oxalic acid by heating paraffin with $HNO_3$.[115]

The most underestimated chemical feedstock of our times might be $CO_2$. $CO_2$ can be converted to oxalic acid in multiple ways as illustrated in Scheme 3. Two routes proceed via oxalate, which is either produced electrochemically from $CO_2$ directly in non-aqueous electrolytes or via formate coupling. Formate can be obtained from $CO_2$ using electrochemistry in aqueous media or via CO as a substrate. Oxalate is then electrochemically or traditionally acidified to oxalic acid. In another route, dimethyl oxalate is produced from CO, which can be obtained from $CO_2$ in various ways described in chapter 4.1 below. Dimethyl

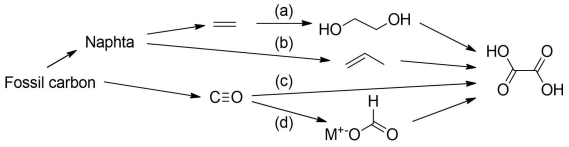


**Scheme 2.** Fossil carbon can be converted to oxalic acid via four pathways: (a) naphtha can be converted to ethylene glycol (via ethylene), which can be oxidized to oxalic acid; (b) propylene is obtained from naphtha cracking and can be converted to oxalic acid; (c) fossil carbon is converted to CO in a gasification process, which can be converted to oxalic acid via the dialkyl oxalate process; and alternatively (d) CO can be converted to formate, which is turned into oxalic acid using formate coupling followed by an acidification step.

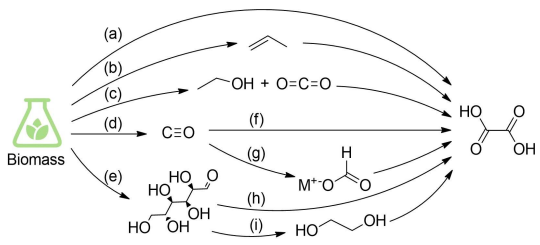


**Scheme 1.** Biomass can be (a) directly converted into oxalic acid by oxidation or used as a feedstock for oxalic acid precursors including (b) propylene, (c) ethanol and $CO_2$, (d) CO, and (e) glucose. CO can be converted into oxalic acid (f) directly or (g) via the formation of formate. Glucose can be (h) oxidized directly or (i) first converted to ethylene glycol, which is subsequently oxidized.

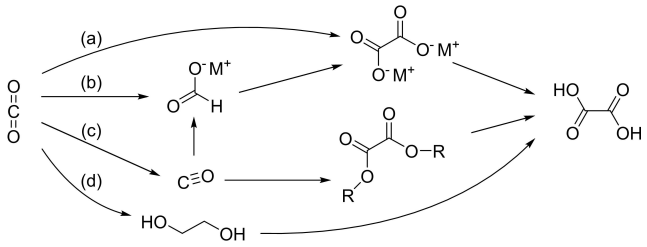


**Scheme 3.** $CO_2$ can be converted to oxalic acid via four main pathways: (a) through direct conversion of $CO_2$ to alkali oxalate; (b) through a metal formate intermediate, which can be obtained from the electrocatalytic or photocatalytic reduction of $CO_2$; (c) via CO and the dialkyl oxalate process; and (d) via ethylene glycol and subsequent oxidation (in practice not done because ethylene glycol would be obtained from oxalic acid, not vice versa).

oxalate is then hydrolyzed to oxalic acid. Ethylene glycol can also be obtained from $CO_2$ and oxidized to oxalic acid.

$CO_2$ is mainly known for the environmental problems it causes, which include climate change and ocean acidification.[116] To become truly circular and mitigate these problems, the utilization of $CO_2$ as a feedstock is required as some $CO_2$-emitting sources such as cement, steel, or ammonia production cannot be avoided or using a carbon source is strongly preferred even though alternative processes using hydrogen were proposed. For the industry to develop and adopt $CO_2$ as a feedstock, however, it also requires processes (and regulations or taxes) to be competitive in the market to compete with and limit the dependency on fossil fuels.[12,21,117] Obtaining it directly from the air using so-called direct air capture processes is difficult due to the low $CO_2$ concentration (400 ppm in the air) and requires high energy input.[118] Today, high-purity industrial point sources, such as carbohydrate fermentation to methanol, natural gas processing, hydrogen production from methane, coal/gas-to-liquids, steel, and cement production, energy generation, and ammonia production, supply the majority of the $CO_2$ that is injected in $CO_2$ storage demonstration projects.[119] $CO_2$ can be captured relatively cheaply in large-scale cement or steel factories.[120,121] The publications on $CO_2$ conversion are at an all-time peak, indicating high scientific interest.[122]

## 3. Direct Conversion of $CO_2$ to Oxalic Acid

Ideally, we should directly convert $CO_2$ into oxalic acid in one step. $CO_2$ can be obtained directly from the air or point sources. Several reviews on $CO_2$ capture technologies and their implications are available.[123–127] There are many routes for direct reduction of $CO_2$, which can be summarized in three categories as shown in Scheme 4. They include (a) direct classic electrochemical $CO_2$ reduction catalyzed by metals, (b) electrochemical reduction catalyzed by metal complexes, and (c) sacrificial reduction with calcium ascorbate. None of these processes are in the commercial stage yet due to low yields, low turnover numbers, or the high complexity of the systems. For example, former Princeton spin-off Liquid Light (now Avantium) developed an electrochemical one-step route to oxalate, but the requirement of a stable nonaqueous electrolyte proved to be a barrier to scale-up.[128]

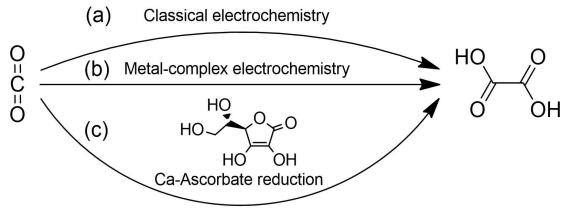


**Scheme 4.** Direct conversion of $CO_2$ to oxalate followed by acidification to oxalic acid: (a) direct electrochemistry; (b) $CO_2$ reduction catalyzed homogeneously by metal complexes; (c) reduction of $CO_2$ with Ca-ascorbate and electrochemical regeneration.

### 3.1. Direct electrochemical $CO_2$ reduction

Electrochemical reduction is a powerful means to activate and convert $CO_2$, but it is also challenging. A comprehensive overview of all aspects of electrochemical reduction of $CO_2$ on metal electrodes is available from Hori.[129] The nature of the formed product crucially depends on the reaction medium and choice of electrode material.

Ikeda et al. proposed that the $CO_2$ reduction reaction proceeds via single-electron reduction leading to the formation of a $CO_2^{\bullet-}$ radical anion.[130] The formed $CO_2^{\bullet-}$ radical anion is highly reactive and reacts with proton donors such as water to form undesired formate and carbonate following Equation (1). Therefore, the choice of the reaction medium is of great importance.[131–134]

$$2\ CO_2 + H_2O + 2e^- \rightarrow HCO_2^- + HCO_3^- \quad (1)$$

This unwanted side reaction can be suppressed when solvents of low proton availability are used. If the $CO_2^{\bullet-}$ anion radical is present long enough on the electrode surface, it reacts with another one, and oxalate is formed as shown in Equation (2). This mechanism has been proven with in-situ spectroscopy by Eneau-Innocent et al.[135]

$$2\ CO_2 + 2e^- \rightarrow 2\ CO_2^- \rightarrow C_2O_4^{2-} \quad (2)$$

The formation of the $CO_2^{\bullet-}$ radical anion is thermodynamically unfavored due to large reorganizational energy between the linear molecule and bent radical anion.[136] In practice when using dimethylformamide, the uncatalyzed reaction required standard potential is −2.21 V vs. saturated calomel electrode.[137] A large standard potential can lead to large operation potentials, which should be avoided as they reduce the process efficiency. Metal catalysts can lower the standard potential by providing alternative reaction pathways and subsequently allow for a lower overall operation potential of $CO_2$ activation.

Tin, mercury, lead, indium, and tellurium electrodes proved suitable for the reaction in an early stage, and oxalic acid was produced at 90% faradaic efficiency (FE) in dimethyl formamide.[130,134,138] Newer developments include the use of metal oxides such as $MoO_2$ in combination with lead electrodes.[139]

If the radical anion is not staying on the surface it migrates into the electrolyte where it can react with another $CO_2$ to form CO and $CO_3^{2-}$ via reductive disproportionation according to Equation (3), rather than to oxalate according to Equation (2).[140] Electrodes made from platinum, palladium, gold, or copper favor this unwanted side reaction.[130,141]

$$2\ CO_2 + 2e^- \rightarrow 2\ CO_2^- \rightarrow CO + CO_3^{2-} \quad (3)$$

In conclusion, three competing reactions [Eqs. (1–3)] are present during the direct electrochemical reduction of $CO_2$ to oxalic acid.[137] The absence of water is crucial as it does not only favor formate production but also further the reduction of oxalate to glycolate.[131,132] Although it is beneficial to have

trace amounts of water present if $CO_2$ is reduced to CO, this is not the case if oxalic acid is desired.[142] Therefore, the absence of water, even in trace amounts, is critical to achieving high FEs.[143] Kaiser and Heitz were the first to develop a suitable process and considered parameters such as electrode materials, solvents, pH, and current densities.[131] Propylene carbonate, acetonitrile, and dimethylformamide were found to be the most suitable solvents due to their relatively low nucleophilicity at a sufficient electrophilic constant. Adding tetraethylammonium perchlorate as a supporting electrolyte was found to increase oxalate production by improving electrochemical contact between $CO_2$ and the working electrode surface.[144] Recently also the reaction temperature was added to the list of important reaction conditions.[145] In some instances, a low reaction temperature as low as $-20\,^{\circ}C$ can be beneficial to help suppress hydrogen evolution from water splitting in wet organic solvents such as acetonitrile and dimethylformamide.[139]

A commercial industrial process called the zinc oxalate process was developed by Heitz and co-workers. The use of a sacrificial zinc anode forms insoluble zinc oxalate, which can be removed from the electrolyte by simple filtration.[146,147] As a first step, $CO_2$ is reduced to oxalate as in Equation (4); at the same time zinc is oxidized to $Zn^{2+}$ [Eq. (5)]. Together they form insoluble zinc oxalate [Eq. (6)]. After filtration, the oxalate can be acidified with sulfuric acid, where oxalic acid and zinc sulfoxide are formed following Equation (7). The zinc and sulfuric acid can be recovered by electrolysis in water as in Equation (8). Overall, oxalic acid is obtained from $CO_2$ and water as in Equation (9).[146]

Oxalate electrolysis:

$$2\ CO_2 + 2e^- \rightarrow\ C_2O_4^{2-} \tag{4}$$

$$Zn \rightarrow Zn^{2+} +\ 2e^- \tag{5}$$

$$2\ CO_2 + Zn \rightarrow\ ZnC_2O_4^{2-} \downarrow \tag{6}$$

Oxalic acid from zinc oxalate:

$$ZnC_2O_4 + H_2SO_4 \rightarrow ZnSO_4 +\ H_2C_2O_4 \tag{7}$$

Zinc electrolysis:

$$ZnSO_4 +\ H_2O\ \rightarrow Zn +\ H_2SO_4 + \frac{1}{2}\ O_2 \tag{8}$$

Sum of all reactions:

$$2\ CO_2 +\ H_2O\ \rightarrow H_2C_2O_4 + \frac{1}{2}\ O_2 \tag{9}$$

The overall process requires four cycles as shown in Figure 4. The advantages of the process are high current efficiencies (>90%) and the absence of unwanted side products and precious metals in the process. Economic calculations lead to the conclusion that the process is price competitive on a 2 million ton scale. A disadvantage is the need for dry organic solvents. Unfortunately, the process has never been tested on the pilot stage as a continuous close-loop operation.

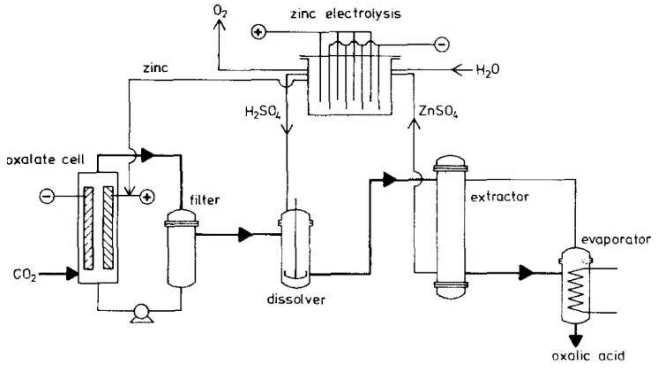


**Figure 4.** Flow sheet of zinc oxalate process as developed by Fischer et al. In the bottom left in the first cycle, $CO_2$ is converted to zinc oxalate and removed by filtration. The oxalate is dissolved in sulfuric acid in the second cycle, and oxalic acid is extracted from the zinc sulfate solution, which is recycled to sulfuric acid and zinc in the zinc electrolysis cell shown at the top. Pure oxalic acid is obtained by evaporation of the extractant in the last step in the bottom right. Reproduced with permission from Ref. [147]. Copyright 1981, Springer.

Most recently Paris and Bocarsly reported a new system operating in aqueous media.[148] It comprises a thin film of alloyed Cr and Ga oxides on glassy carbon, which electrocatalytically generates oxalate from aqueous $CO_2$ with a maximum oxalate FE of 59% at potentials as positive as $-0.98$ V vs. normal hydrogen electrode (NHE).

Oxalate is produced at a surface anion site via a CO-dependent pathway instead of relying on the formation of a $CO_2^{\bullet-}$ radical anion, hence the reduced need for non-protic environments. However, the catalysts exhibit two sites, which can either favor oxalate or formate formation. To favor oxalate production the crucial parameters such as pH, alloy ratio, and electrolyte cation need to be optimized. A pH of 4.1 with KCl as electrolyte and a $Cr_2O_3/Ga_2O_3$ ratio of 3:1 was shown to be most favorable. This process is still in a very early stage and still needs to prove scalability.

### 3.2. Metal-complex electrocatalysis

Homogeneous catalysts have a long history in $CO_2$ reduction of over 40 years. However, the primary interest was the formation of syngas or the direct formation of possible fuels. A comprehensive Review on the topic has been published by Benson et al.[136] Some groups also focused on the production of oxalate. Becker et al. were the first to develop homogeneous catalysts specifically for the formation of oxalate.[149] They made use of silver and palladium porphyrins and were able to drop the operation potential from $-2$ to $-1.5$ V and found selectivity towards oxalic acid in absence of CO. They did not state any selectivity or efficiency numbers and possible mechanisms.

Kushi et al. had a different approach and made use of a rhodium sulfide cluster in $CO_2$-saturated $CH_3CN$ in the presence of $LiBF_4$ as shown in Figure 5.[152] They could also lower the operation potential to −1.5 V whilst operating at 60% current efficiency. The cluster was crafted on a glassy carbon plate and did not show any signs of fragmentation. Not only low-valence metal but also electron-rich sulfur ligands are the possible sites for the activation of $CO_2$ by metal-sulfur clusters. Fourier-transform (FT)IR studies revealed the presence of $CO_2$ bonded to the reduced clusters at either two Rh or a S and Rh site.

In a subsequent study, they could show even better activity using iridium and cobalt complexes with which the operation potentials could be lowered to −1.3 and −0.7 V, respectively, whilst maintaining 60% current efficiency. This resembles a strong decrease of the overpotential of 1.4 V compared to the uncatalyzed reaction.[150]

Evans et al. were up next and demonstrated the use of lanthanides, in this case samarium, as a suitable catalyst to reach high selectivity of oxalic acid in appropriate conditions.[151]

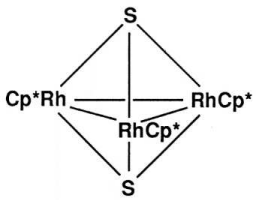


**Figure 5.** Structure of the triangular rhodium complex $[(RhCp^*)3(\mu3\text{-}S)_2]^2$. Reproduced with permission from Ref. [152]. Copyright 1994, The Chemical Society of Japan.

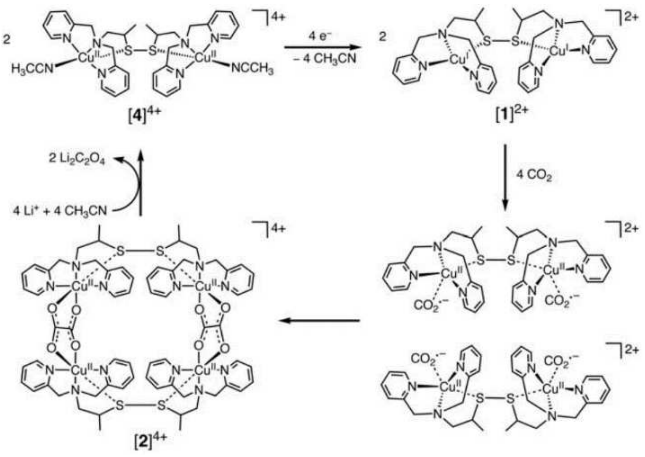


**Figure 6.** Catalytic cycle of copper complex for $CO_2$ activation as proposed by Bouwman and co-workers. The initial copper(II) complex $[4]^{4+}$ is first reduced at −0.03 V vs. NHE to the copper(I) complex $[1]^{2+}$. This is subsequently reduced by two $CO_2$ to copper (ii) again. Two of the complexes merge and the bound $CO_2^{\bullet-}$ radical anions couple to form bridging oxalate molecules $[2]^{4+}$. Lithium ions and acetonitrile liberate the oxalate as lithium oxalate and the initial complex is formed again. Reproduced with permission from Ref. [153]. Copyright 2010, American Association for the Advancement of Science.

In 2010 Bouwman and co-workers first described a dinuclear copper(I) complex that is oxidized by $CO_2$ rather than by $O_2$ when brought into contact with air.[153] The $CO_2$ is captured and a tetranuclear oxalate-bridged copper(II) complex is formed as shown on the bottom left of Figure 6. The captured oxalate can be then liberated as oxalic acid by the addition of hydrochloric acid.

Alternatively, the authors developed a system in which lithium perchlorate is used as a supporting electrolyte and acetonitrile as solvent. This system allows for a full catalytic cycle as shown in Figure 6. First the copper(II) complex $[4]^{4+}$ is reduced to the copper(I) complex $[1]^{2+}$, which is then oxidized by two $CO_2^{\bullet-}$ molecules, which are bound as $CO_2^{\bullet-}$ radical anions. Two of the complex pairs form the oxalate-bridged tetranuclear copper(II) complex $[2]^{4+}$. The complexed oxalate then is liberated by the lithium ions as lithium oxide and acetonitrile refills the vacant coordination spaces of the complex.

Preliminary results demonstrate six turnovers (producing 12 equiv. of oxalate) during 7 h of catalysis at an applied potential of −0.03 V vs. NHE. However, no yields or selectivity were reported, and the coverage of the electrode with precipitated oxalate leads to deactivation as it hampers efficient electron transfer.

In 2014, Maverick and co-workers presented a copper complex for $CO_2$ transformation to oxalate but have retracted that article recently.[154,155]

They had initially introduced ascorbic acid as mild reducing agent, which has been long known to decompose to oxalates in the presence of transition metals and oxygen. Now they identified the reducing agent as the source of oxalate rather than the reduction of $CO_2$. The reduced $Cu^{I}$ complex does react with $CO_2$ but forms a stable carbonate complex instead (Figure 7)

Kumar et al. used a different approach for the special organization of their catalyst and designed a copper-based metal-organic framework (MOF).[156] They could decrease the overpotential by 0.7 V and increase the current density from 2.27 to 19.22 mA cm$^{-2}$ in DMF solution and Tetrabutylammonium tetrafluoroborate (TBATFB) as supporting electrolyte. They proposed the formation of the $CO_2^{\bullet-}$ radical anion, which couples to oxalate and then abstracts a proton from the solvent to form oxalic acid with 90% selectivity at 51% FE.

The advantages of transition metal complex systems are their high selectivity and the use of non-precious metals in some examples. However, the low FE, long reaction times, and use of toxic solvents are major drawbacks. In addition, the process development suffers from highly complex systems and is hence at an early stage of development on a lab scale. The recent retractions emphasize the challenges and complexity of these systems further.

### 3.3. Sacrificial reduction using Ca-ascorbate

The work of Pastero et al. shows that also pathways without harmful reagents, complicated metal complexes, or electro-

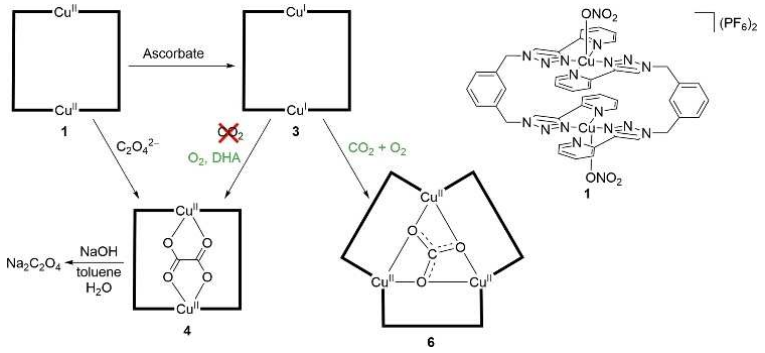


**Figure 7.** Revised version of the original three-step reaction cycle for reduction of $CO_2$ to oxalic acid. The starting $Cu^{II}$ complex (**1** or **2**) is reduced to a $Cu^{I}$ complex by sodium ascorbate (**3**). In the presence of oxygen, the ascorbate is reduced to oxalate to give oxalate-bridged complex (**4**). In the presence of $CO_2$ and absence of ascorbate, however, a stable three-valent carbonate complex is formed. Reproduced with permission form Ref. [155]. Copyright 2021, Nature Publishing Group.

chemical cells are available.[157] They made use of the oxidizing potential of the calcium salt of ascorbic acid (AA), more widely known as Vitamin C. They claim that AA is not only nontoxic but also cost-effective as a reducing agent, citing its earlier applications in the biomedical and food industry.

AA is unstable in solution and decomposes to dehydroascorbic acid as shown in Equation (10) with a redox potential of 0.5 V vs. NHE.[158]

$$C_6H_8O_6 \rightarrow C_6H_6O_6 + 2\,H^+ + 2\,e^- \quad (10)$$

In their experiments, stoichiometric amounts of calcium AA salt react with the $CO_2$ to form insoluble calcium oxalate in the form of Weddellite-type crystals. The reaction rate was found to be depending on pH, temperature, and reactor design but optimal conditions were not presented. Advantages of this process are the simple equipment and absence of precious metal catalysts. However, the stoichiometric consumption of AA is a major drawback as AA requires a complicated multistep production process and therefore has a much higher market price than the product oxalic acid.[159] Additionally the sacrificial $CO_2$ process is yet to be tested on a larger scale.

## 4. Carbon Monoxide to Oxalic Acid

Carbon monoxide can be used as a feedstock for oxalic acid in various ways. It is mainly used indirectly to produce feedstock for oxalic acid production, but the direct pathway is also possible via the dialkyl oxalate as shown in Scheme 5.[160,161]

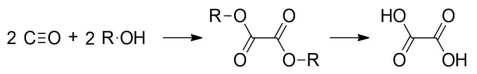


**Scheme 5.** CO can be converted to oxalic acid via the dialkyl oxalate process, where first the dialkyl ester of oxalic acid is formed, which is then hydrolyzed to oxalic acid.

### 4.1. Carbon monoxide production

Carbon monoxide is a toxic gas generated mainly by the incomplete combustion of carbon compounds.[162] It was first isolated in 1776 by de Lassone and is increasingly used as feedstock on a very large scale in the chemical industry, as a pure reactant for the production of hydrogen (water-gas shift reaction), inorganic chemicals, and acetic, acrylic, or propanoic acid in the Cativa process.[163] In conjunction with hydrogen, it is called syngas and used for the production of alcohols, hydrocarbons, or linear aliphatic aldehydes using the process.[164]

All production pathways of CO are illustrated in Scheme 6, including those from the most common source in commercial quantities, which is still fossil carbon.[162] This includes the gasification of coal, steam reforming, the Boudouard reaction, and the partial oxidation of hydrocarbons.[162] Alternatively, CO can be obtained from the thermal treatment of biomass or $CO_2$. CO can be produced from $CO_2$ using heterogeneously catalyzed reverse water-gas shift reaction, electrochemically, or photochemically.[165–168]

#### *4.1.1. Fossil carbon conversion*

The major industrial process for the production of CO is the Boudouard reaction in which $CO_2$ from fossil carbon combus-

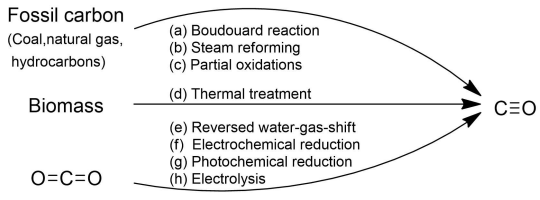


**Scheme 6.** CO can be obtained from fossil carbon, biomass, and $CO_2$. Fossil routes include (a) Boudouard reaction, (b) steam reforming of gas, and (c) partial oxidation of hydrocarbons. Biomass can be (d) thermochemically converted and $CO_2$ can be reduced to CO via (e) reverse water-gas-shift reactions, (f) direct electrochemical reduction, or (g) electrolysis.

tion [Eq. (11)] reacts with carbon [Eq. (12)]. Above 800 °C, CO is the predominant product:

$$C + O_2 \rightarrow CO_2 \quad (11)$$

$$C + CO_2 \rightarrow 2\ CO \quad (12)$$

Through this reaction, $CO_2$ from a variety of combustion plants can be upgraded to CO, but the process is energy intensive.[169] In the gasification of coal, both CO and hydrogen are formed [Eq. (13)], which requires separation.

$$3\ C + O_2 + H_2O \rightarrow 3\ CO + H_2 \quad (13)$$

The steam-reforming process, discovered by Fontana in 1780, only uses water and no additional oxygen as in Equation (13). This leads to a higher proportion of hydrogen in the mix:

$$C + H_2O \rightarrow CO + H_2 \quad (14)$$

In partial oxidation, CO is produced from natural gas or heavy hydrocarbons and a limited amount of oxygen to form CO and hydrogen [Eq. (15)].

$$C_nH_m + \frac{n}{2}O_2 \rightarrow n\ CO + \frac{m}{2}H_2 \quad (15)$$

The advantage of these processes is that they are all technically mature and have been used commercially for many decades. However, to be sustainable the fossil feedstock has to be replaced with a sustainable carbon source. A further disadvantage is that these processes all produce gas mixtures, which should be separated in various processes by reversible complexation, cryogenic separation, pressure swing adsorption, or permeable membranes. All of these require extensive equipment and significant energy. Alternatively, CO can be produced from biomass or $CO_2$, which will be described in the next section.

#### *4.1.2. Thermal biomass conversion*

The production of CO from biomass is possible from various sources, but algae are especially suitable due to their simple cell structure and composition.[170–172] All routes in principle are thermochemical conversion of the biomass in the form of either pyrolysis, gasification, or direct combustion.[171] Those routes are described and discussed by Lam et al.[172] The resulting gas mixture requires gas separation similar to fossil processes.

#### *4.1.3. Reverse water-gas shift*

The reverse water-gas shift reaction was first discovered by Bosch and Wild in 1913 and is commercially used for methanol synthesis and syngas processes.[173,174] It is equilibrium limited and favored at high temperatures as it is endothermic [Eq. (16)].

$$CO_2 + H_2 \rightarrow CO + H_2O \quad (16)$$

For the hydrogen route to be sustainable, the hydrogen must be produced via electrochemical water splitting.[175] The reaction is usually carried out in simple single-stage adiabatic reactors with the help of supported metal catalysts of which iron- and copper-based catalysts are most common.[166,176–179] An in-depth introduction on the reaction, reactor, and catalyst design was published by Newsome.[179] Daza and Kuhn discussed the recent developments in catalysts and mechanisms and their consequences on economics in great detail in their 2016 Review.[165] This path of CO production has the advantage of scalability, high selectivity towards CO, and a simple process design. However, catalysts that are highly selective at high production rates are yet to be found.[165]

#### *4.1.4. Electrochemical reduction of $CO_2$*

The electrocatalytic $CO_2$ reduction reaction as in Equation (17) is considered one of the most attractive methods of storing intermittent renewable energy as chemical energy on a large scale.[24]

$$CO_2 + 2\ H^+ + 2\ e^- \rightarrow CO + H_2O \quad (17)$$

Although a vast variety of products are accessible through the electrocatalytic $CO_2$ conversion pathways, only CO and formic acid/formate ($pK_a = 3.77$) are produced at high FEs (above 80%) and current densities above 100 mA cm$^{-2}$ for hundreds of hours.[180,181] The formation of $CO_2$ proceeds via the formation of a $CO_2^{\bullet-}$ anion radical as described above. The choice of a protic solvent favors the production of CO over oxalate. The choice of the metal determines whether formate or CO is formed.[129] A recent review from Nielsen et al.[182] provides a good overview of the electrochemical $CO_2$ reduction process, and several other authors discuss various aspects in great detail.[116,165,167,175,180,183–187] Hernández et al. and Chen et al. discussed the options in a broader scope, evaluated the state of the art results, and came to the conclusion that whilst the development of the direct electrochemical processes has progressed significantly, they still have challenging obstacles to overcome before becoming industrially viable.[183,184] Overall, the advantage of these processes is the use of gaseous $CO_2$ and renewable energy as a feedstock. Due to fluctuations in the availability of renewable energy, the short start-up time of these systems may be an advantage. Disadvantages are the use of precious metals as catalysts and complex electrode designs, which make long-term stability, production rate optimization, and upscaling challenging. Large-scale demonstrators yet need to show the viability of this process.

#### 4.1.5. Photochemical $CO_2$ reduction

The production of CO from $CO_2$ using photochemical cells is similar to the photochemical production of formate as described below and discussed in recent Reviews by Das and Daud and Saravanan and co-workers.[188,189]

The advantage here is the direct harvesting of sunlight and the ambient reaction conditions at which the reaction takes place. However, complex reaction systems and difficult reactor design pose challenges for commercialization. Hence, existing techniques are yet insufficient for industrial application and further research into solar-driven photocatalysts is required.[188]

#### 4.1.6. High-temperature conversion

At high temperatures, $CO_2$ can be converted to CO and oxygen as in Equation (18). The reaction can be either performed as electrolysis using solid oxide electrolyzer cells or purely thermochemically at 900 °C on metal oxides as catalysts with high oxygen mobility.[167,190–193]

$$2\ CO_2 \rightarrow 2\ CO + O_2 \tag{18}$$

The advantage of this process is that only $CO_2$ is needed as a reactant, but the major drawback is the high temperature, which requires special equipment and high heat input, still with rather slow reaction rates. Commercial systems for solid oxide electrolysis are already available.[194]

### 4.2. CO to oxalic acid: the dialkyl oxalate process

In 1974 Fenton et al. were the first to describe the liquid-phase synthesis of dialkyl oxalate by oxidative carbonization of CO with ethanol and $O_2$ in the presence of a $PdCl_2$-$CuCl_2$ catalyst in the liquid phase.[161]

The first step is the oxidative CO coupling reaction with aliphatic alcohol under the influence of a palladium catalyst to produce the oxalate diester [Eqs. (19–22)].[161]

$$2\ CO + 2\ ROH\ + PdCl_2 \rightarrow (COOR)_2 + 2\ HCl + Pd_0 \tag{19}$$

$$Pd_0 + 2\ CuCl_2 \rightarrow PdCl_2 + Cu_2Cl_2 \tag{20}$$

$$Cu_2Cl_2 + 2\ HCl\ + \frac{1}{2}\ O_2 \rightarrow 2\ CuCl_2 + H_2O \tag{21}$$

$$\text{Overall}:\ 2\ CO + 2\ ROH\ + \frac{1}{2}O_2 \rightarrow (COOR)_2 + H_2O \tag{22}$$

The prepared dialkyl oxalate is hydrolyzed to oxalic acid and the corresponding alcohol [Eq. (23)].

$$(COOR)_2 + 2\ H_2O \rightarrow (COOH)_2 + 2\ ROH \tag{23}$$

This method requires a large amount of dehydrating agent to remove water, which is formed in this reaction step and acts as an inhibitor.[161]

UBE Industries (Japan) patented a two-step process to prepare dialkyl oxalate in 1974.[113] This step was taken after improving the reaction by the introduction of alkyl nitrates as re-oxidizing agents for the palladium catalysts supported on carbon. Improvements include increased reaction efficiency and catalyst lifetime whilst operating at lower temperatures.[195] An added advantage is the role of a dehydrating agent of the alkyl nitrates.[109] The most beneficial nitrate was found to be *n*-butyl nitrate.[110] Further studies have elucidated the role of the catalyst support and ideal catalyst compositions for the reaction.[112,196] The process as shown in Figure 8 is used since 1978 to produce oxalic acid as a starting material to produce fine chemicals.[197]

The process, which is well described in vast detail in the Review by Uchiumi et al., has the advantage of high selectivity, mild reaction conditions, efficient utilization of raw material, and high product quality.[195]

## 5. Formate/Formic Acid to Oxalic Acid

The production of oxalic acid via the formate coupling route (Scheme 7) is one of the oldest processes and has been one of the primary ways to produce oxalic acid before the advent of petrochemistry.[160,198,199]

### 5.1. Production of formate

Formate can be produced either directly from $CO_2$ or CO, the latter of which allows to tap into a broad variety of feedstocks as described above. All routes are shown in Scheme 8 and include the commercial route from CO and hydroxides, hydrogenation of carbonates, and direct electrocatalytic, photochemical, or enzymatic reduction of $CO_2$.

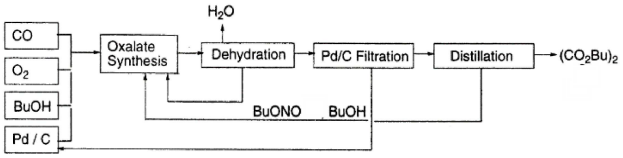


**Figure 8.** Flow diagram of UBE liquid phase process for oxalic acid production in $(CO_2Bu)_2$. Reproduced with permission from Ref. [195]. Copyright 1999, Elsevier.

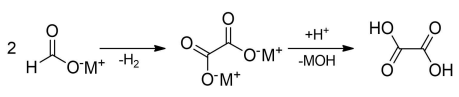


**Scheme 7.** Alkali formates can be converted to oxalic acid via formate coupling to oxalate and subsequent acidification to oxalic acid.

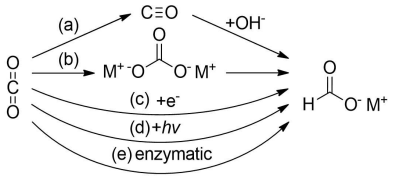


**Scheme 8.** Alkali formates can be obtained directly or indirectly from $CO_2$. The two indirect ways include (a) CO reduction with caustics and (b) hydrogenation of carbonates. The direct conversion of $CO_2$ can be either (c) electrochemical, (d) photochemical reduction, or (e) enzymatic conversion.

#### *5.1.1. Formate from CO and caustic alkali*

Today's commercial route to formate as shown in Equation (24) uses CO and caustic alkalis such as potassium hydroxide. This was first discovered by Berthelot in 1856 and first turned into a commercially viable process by Weise et al.[200,201]

$$CO + MOH \rightarrow HCOOM \tag{24}$$

CO and the caustic alkalis react in an aqueous solution to yield the corresponding formates. In today's commercial plants, the CO is mixed counter-currently with aqueous alkali hydroxide in a tower reactor at 1.5–1.8 MPa and 180 °C, leading to the formation of alkali formate. The process is beneficial if surplus hydroxide can be used for the process.[202]

#### *5.1.2. Carbonate hydrogenation*

An alternative route to formate is the catalytic transformation of $CO_2$, which can be achieved by hydrogenation of bicarbonate in an alkaline environment [Eq. (25)].[203]

$$HCO_3^- + H_2 \rightarrow HCO_2^- + H_2O \tag{25}$$

Carbonate or bicarbonate can be obtained from the reaction of $CO_2$ with alkaline minerals by in-situ or ex-situ mineral carbonation with alkaline metals. This reaction also gained interest as a means for CCS as mineral carbonates such as $CaCO_3$ or $MgCO_3$ are the thermodynamically most stable form of carbon.[204] Alternatively, Yu et al. reported the biomimetic enzymatic conversion of $CO_2$ to bicarbonate over functionalized mesoporous silica.[205]

The first synthesis of formates by hydrogenation of in-situ formed carbonates was reported in 1914 by Bredig and Carter, using palladium supported on carbon under relatively mild conditions at 70–95 °C, 30–60 bar of $H_2$, and 0–30 bar of $CO_2$.[206] Since the work focused on avoiding the use of expensive metals as catalysts to decrease the cost of the process, the influence of process conditions and various new metallic catalysts was tested.[203,207–209] Nickel-containing catalysts appear to be the most effective among those tested, giving 77% formate yield.[203] Zhao et al. introduced a catalytic process in which $CO_2$ hydrogenation to formate is carried out in the presence of transition metal-free homogeneous catalyst.[209]

To use this process sustainably, the hydrogen has to come from water splitting.[175] Alternatively, reducing agents or biomass-derived alcohol, polyol, or sugars including isopropanol, glycerol, or glucose can be used as hydride donors.[210]

The use of reducing agents is described in a 2016 patent as a one-pot metal-catalyzed process.[208] Carbonate salts react in a polar solvent such as water or ethanol at 50–90 °C for 6–24 h at atmospheric pressure in the presence of a reducing agent such as $NaNO_3$, $LiAlH_4$, hydrazine hydrate, AA, or $NaBH_4$ and a catalyst such as $CoCl_2$, $TiO_2$, ZnO, CuO, metal-doped-TiCh, or Cu nanoparticles. Formate yields up to 98.98% were reported with sodium nitrate and Aeroxide P90 $TiO_2$ catalyst at 90 °C. The advantages of this process are the mild reaction conditions and high formate yields with precious metal-free catalysts. A disadvantage is the long reaction time. The technology is not yet proven on a commercial scale.

#### *5.1.3. Electrocatalytic reduction of $CO_2$ to formate*

The electrocatalytic $CO_2$ reduction to formate is a two-electron process as shown in Equation (26).[211] The main competing reactions are the formation of CO as in Equation (17) (see above) and the hydrogen evolution reaction as in Equation (27), which depends heavily on the choice of catalyst.[24,212]

$$2\ CO_2 + H_2O + 2e^- \rightarrow 2\ HCO_2^- + \frac{1}{2}\ O_2 \tag{26}$$

$$H_2O + 2e^- \rightarrow H_2 + 2OH^- \tag{27}$$

Catalysts show high $CO_2$ reduction and low hydrogen evolution activity when they exhibit a weak metal-hydrogen bond reaction. They consist of metals typically located at the left-hand branch of Trassati's volcano plot such as silver, tin, lead, mercury, zinc, or indium (Figure 9).[213,214] Bi- or multimetallic systems, which are complex yet easy to produce, are promising candidates for improving selectivity and lowering overpotentials.[215,216] An early mechanistic study by Hori et al. found that the $CO_2$ radical anion is formed first and bound to the tin or indium catalyst via an oxygen atom. Subsequently, the $CO_2$ radical anion on the surface tends to be protonated at the carbon position, leading to the release as formate. Conversely, a $CO_2$ radical anion on the surface of a gold or silver catalyst is bound to the metal via the carbon atom and therefore tends to be protonated/reduced at an O-position, which results in the production of a *COOH intermediate that can be further reduced to CO.[217]

The metals and metal oxides or sulfide-derived catalysts promote the reaction. The oxide layer films of metals, shown on the descending branch of the volcano plot in Figure 9, can inhibit hydrogen evolution.[214,218,219]

The advantage of this process is that gaseous $H_2$ is not required, and the reaction can be catalyzed by non-noble metals. Furthermore, the energy input can be potentially

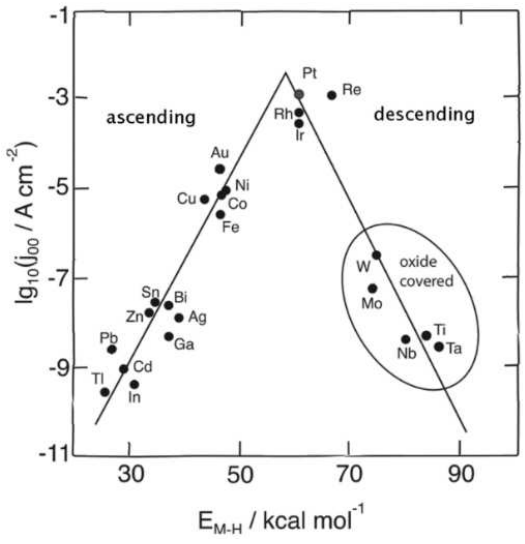


**Figure 9.** Trassati's volcano plot shows the relationship between metal-hydrogen bonding energies (on the *x*-axis) and the exchange current for hydrogen evolution (on the *y*-axis) for several metals. Reproduced with permission from Ref. [219]. Copyright 2014, Beilstein Institut.

supplied from renewable sources such as solar energy.[220] In general, the electrochemical method has several advantages as it is a room-temperature process that favors high selectivity and higher $CO_2$ solubility.

To be economically feasible, the target is to create a system that has a high FE and a high current density, with a catalyst that is stable for a long time. An overview of the implications and new developments on metal catalysts used in the reduction of $CO_2$ to formate is given in the comprehensive Review by Wu et al. and a perspective by Zhang and co-workers.[220,221] Black carbon or salt deposits on metal electrodes have been observed during the electrochemical reduction of $CO_2$.[222] This can result from the further reduction of formate on the catalyst surface if the formate stays in contact with the catalyst for too long. The GLS (gas-liquid-solid) cathode with a gas-through feature can facilitate the removal of the formate products from the catalysts by gas bubbling.[212] The design of the electrodes plays a crucial part in the efficiency of the process. A comprehensive Review by Philips et al. discusses the importance of electrode design and suggests that industrially relevant yields and efficiencies will most likely require gas-diffusion electrodes and intelligent cell designs.[33] Pilot or commercial scale tests are yet to prove the scalability and viability of this process.

#### *5.1.4. Photocatalytic reduction of $CO_2$ to formate*

The photocatalytic reduction of $CO_2$ makes direct use of the sun's power in that the incoming photons are harnessed to drive the reaction and CO and formate are the most commonly obtained products.[223] It is attractive as it is operated at ambient pressure, low temperature, and does not require high input energy.[188] Ideally, the solar energy can be harvested to power a water oxidation catalyst and couple it with a $CO_2$ reduction catalyst with well-controlled product selectivity for the $CO_2$ reduction.[224] This reaction can be facilitated on the surface of semiconducting heterogeneous catalysts, but these systems still suffer from strong catalyst deactivation by deposited formates on the surface.[225–227] Hence, the most common systems for this process are homogeneous catalysts, which have been first used by Tanaka and co-workers in the 1980s.[228] In recent years this topic gained new interest and many new systems were studied and developed.[224,229–235] The selectivity of the homogeneous systems depends on a myriad of parameters in the process design including the solvent for $CO_2$ solubilization, electron and proton sources, photosensitizers for light-harvesting, and lastly the design of the catalysts itself.[224] Figure 10 exemplary shows the complex nature and the reaction cycles for the most advanced system to date.

The developed systems are not yet competitive on a commercial scale.[189] They lack energy efficiency, catalyst stability, and selectivity towards formate, for which a maximum of 65% was achieved by Delcamp and co-workers.[224] The slow reaction rates, intermittency of light, and high equipment cost due to its complexity are further drawbacks.[236,237] Two comprehensive Reviews by Saravanan and co-workers and Das and Daud give an excellent overview of available catalytic systems, recent developments, and possible reactor designs.[188,189]

#### *5.1.5. Enzymatic conversion of $CO_2$ to formate*

The first enzymatic catalytic formate production was reported by Pereira and co-workers, who used a whole-cell approach

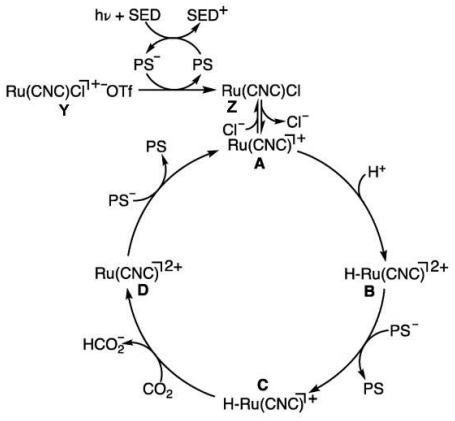


**Figure 10.** Proposed mechanism for formate production under the influence of Ru catalyst and hydrous conditions. The cycle begins at the top left with the pre-catalyst **Y**, which is activated by the electron transfer from the sacrificial electron donor (SED) to the photosensitizer (PS) to yield **Z**. With the dissociation of $Cl^-$, the active catalyst **A** becomes available. **A** chemically transforms by complexation with a proton to form **B**. The dicationic complex **B** subsequently is reduced again by the PS to form **C**, which can react with $CO_2$ to form formate and the dicationic complex **D**. Reduction of the dicationic complex **D** by the PS regenerates the initial complex **A**. Reproduced with permission from Ref. [224]. Copyright 2019, American Chemical Society.

with the sulfate-reducing bacteria *D. desulfuricans*.[238] These bacteria are ideal for the reaction due to their high expression levels of formate dehydrogenase (FDH) and hydrogenase (Hase), which catalyze the formate production from $CO_2$ and $H_2$, respectively [Eqs. (28) and (29)].

$$CO_2 + 2\ e^- + H^+ \rightleftarrows HCOO^- \quad (28)$$

$$H_2 \rightleftarrows 2\ H^+ + 2\ e^- \quad (29)$$

The use of FDH for $CO_2$ utilization has been widely studied and a comprehensive summary was published by Amao.[239] Two classes of FDHs exist, which depend either on a co-factor such as nicotinamide adenine dinucleotide (NADH) or metals as electron donors and acceptors.[240] Both types are used in $CO_2$ reduction processes. The use of pure enzymes requires highly purified proteins of high functionality, and it is essential to purify and handle the proteins under strictly anaerobic conditions, making their commercial application costly.[241] The stability and activity of FDH can be improved by immobilization on a support such as hollow-fiber microreactors.[242–244]

The metal-dependent FDHs are used in enzymatic electrosynthesis and were discussed in great detail in a recent Review by Zhu and co-workers.[245] Enzymatic electrosynthesis combines enzymatic catalysis and electrochemical techniques by immobilizing the enzymes on electrode surfaces. High FE of 99% was reported at low overpotentials of −0.66 V vs. NHE but reaction rates and current densities were still low; however, this is still in an early stage of development.[240,246]

The reaction with cofactor-dependent FHDs eliminates the need for protons and follows Equation (30).

$$CO_2 + NADH \xrightarrow{FDH} HCOO^- + NAD^+ \quad (30)$$

The cofactors can be recycled photocatalytically with a pristine $TiO_2$ catalyst or electrochemically on copper foam electrodes. Both regeneration types were coupled with the enzymatic reactor in a semi-batch and continuous process.[247,248] In the optimized systems formate yields of up to 80% were reported, highlighting the benefit of the coupled system. However, the achieved reaction rates and scale are still far from commercial needs.

### 5.2. Oxalic acid production via formate coupling

The coupling of formate was first reported by Merz and Weith in 1882.[249] They found that oxalate can be produced by heating various metal formates above 400 °C in the absence of air or oxygen [Eq. (31)].

$$2\ HCOOM_{(s,l)} \xrightarrow{\Delta} M_2C_2O_4 + H_{2(g)} \quad (31)$$

The heating leads to mixed salts containing more than 70% oxalate with carbonate as the main side product. Two side reactions can occur. In 1823, Gay-Lussac discussed the stability of oxalic acid, and already then, the low decomposition temperature of 110–130 °C was reported.[250] The thermal decomposition of oxalate leads to the formation of carbonate and CO. Although more stable than oxalic acid, the formate and oxalate salts can decompose to carbonate and CO as in Equation (32) and (33).

$$2\ HCOOM \rightarrow M_2CO_3 + H_2 + CO \quad (32)$$

$$M_2C_2O_4 \rightarrow M_2CO_3 + CO \quad (33)$$

Merz and Weith found that the amount of carbonate increases with decreasing reaction temperature.[249] Shortly after its discovery, this process became one of the main commercial ways of oxalic acid production, and several processes covering various reactor designs and reaction conditions were patented around the world in the period 1900–1936.[200,251–264] Scientifically, the reaction kinetics, mechanism, and process optimization were first extensively studied by Freidlin et al. at the beginning of the 20th century. He published at least 14 papers on the topic.[265–278] In the 1970s and 1980s, Shishido and Masuda in Japan and Górski and Kraśnicka in Poland investigated the coupling reaction focusing on the different gaseous products from formate decomposition concerning the solid reaction products.[279–284] The most recent mechanistic study was published by us in 2021.[63,285]

Not all formate salts are suitable for oxalate production as many undergo decomposition to carbonates, metal oxides, or metals.[284] Only alkali metal formates can be converted to corresponding oxalates in a coupling reaction. Lithium formate is a major exception to the formate decomposition series. The main products of lithium salts decomposition are CO and lithium carbonate.[276,286] The metal counter ion determines the temperature ranges in which formates are converted into oxalate. Freidlin et al. studied several formates and reported the optimal reaction temperatures for each and associated oxalate yields (Table 1).

Cesium formate is the most thermally stable. It requires the highest temperature of 494 °C to reach a mere 25% oxalate yield.[266] The slightly cheaper rubidium formate requires a lower temperature of 470 °C to reach an oxalate yield of 49 and 66% without and with base catalysts.[272,287] Sodium and potassium formate give much higher oxalate yields of 91 and 82%, respectively, and therefore we only focus on those formates below. The highest oxalate yield with sodium formate can also be achieved at the lowest temperature of 389 °C.[271] However, other authors report higher oxalate yields from potassium formate. Surprisingly, Freidlin reports such high reaction

**Table 1.** Dependence of oxalate yield on formate melting point and optimal reaction temperature (temperature giving highest yield).[266,271,272,275,276]

| Formate | Melting point [°C] | *T* [°C] | Oxalate yield [%] |
|---|---|---|---|
| HCOONa | 253 | 389 | 91 |
| HCOOK | 157 | 455 | 82 |
| HCOORb | 170 | 470 | 49 |
| HCOOCs | 265 | 494 | 25 |
| HCOOLi | 280 | no oxalate formation | |

**Table 2.** Formate coupling catalyzed by hydroxides at reaction temperatures and catalyst loadings at which the highest yields were obtained.[34,273]

| Formate | Hydroxide | *T* [°C] | Catalyst loading [mol equiv.] | Oxalate yield [%] |
|---|---|---|---|---|
| HCOONa | KOH | 341 | 0.032 | 94 |
| HCOONa | NaOH | 330 | 0.050 | 92 |
| HCOONa | NaOH | 390 | 0.042 | 86 |
| HCOONa | KOH | 420 | 0.061 | 78 |
| HCOONa | KOH | 440 | 0.097 | 77 |
| HCOOK | KOH | 410 | 0.111 | 75 |
| HCOOK | NaOH | 411 | 0.135 | 70 |
| HCOONa | KOH | 341 | 0.032 | 94 |

temperatures for potassium formate compared to sodium formate as potassium formate has a much lower melting point. This may be due to a phenomenon described in a patent by Enderli and Schrodt, who suggest that the reaction with potassium formate actually is an equilibrium reaction.[256] Our own studies confirmed this phenomenon, and we will report the underlaying mechanism in an upcoming publication. For future continuous processes, potassium formate has the advantage of a lower melting point. This allows a lower temperature when premixing the formate with catalyst and introducing it to the reactor as a melt.

The basic catalysts increase oxalate yields and decrease reaction times and temperatures. One of the most common bases used commercially is alkali hydroxide, for which varying yields were reported as shown in Figure 11 and Table 2.[34,267,273,289] Hydroxides lower the reaction temperature relative to the uncatalyzed reaction by approximately 50 °C and increase the selectivity to oxalate. The oxalate yield in an industrial process could be drastically increased to 75% using KOH in comparison to 12% for uncatalyzed potassium formate at 410 °C.[273,275]

Unfortunately, hydroxide does not only function as a catalyst but also as a reactant. For each hydroxide molecule added to the reaction, one carbonate is formed [Eqs. (34) and (35)], either from formate or from oxalate, as these reactions require lower temperatures than the coupling reaction.[267]

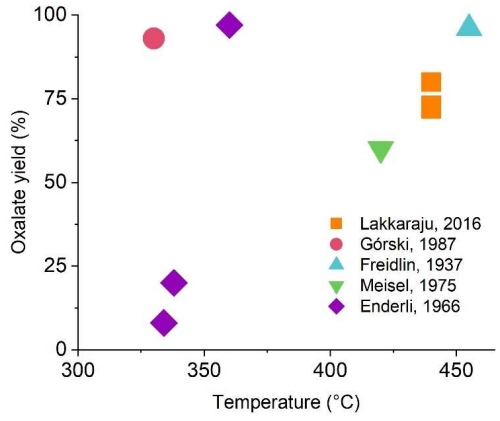


**Figure 11.** Yields of potassium oxalate from KOH-catalyzed reactions as reported in literature and patents.[34,256,281,286,288]

$$HCOOM + MOH \rightarrow M_2CO_3 + H_2 \quad (34)$$

$$M_2C_2O_4 \rightarrow M_2CO_3 + CO \quad (35)$$

The side reactions can be minimized if the reaction is performed in a narrow temperature range due to the slower reaction rates of the side reactions.[273] As the exact mechanisms for these desired and undesired reactions are still unknown, further improvement seems to be feasible as our recent response surface modeling study shows.[290] Freidlin was the first to test alternative bases as catalysts for the reaction (Table 3). He could lower the reaction temperature whilst maintaining or improving the oxalate yield.[270]

Alkali metals are amongst the strongest base chemicals existing.[291] Back in the 1930s, Freidlin et al. studied their effect on the reaction including reaction kinetics and possible mechanisms.[269,278] However, the methodology to estimate the

**Table 3.** Optimal temperatures to produce oxalate from sodium and potassium formates in the presence of various catalysts.

| Formate | Catalyst | *T* [°C] | Oxalate yield [%] | Ref. |
|---|---|---|---|---|
| HCOONa | no catalyst | 390–400 | 91 | [270] |
| | vanadium pentoxide | 370–375 | 92 | [270] |
| | sodium hydroxide | 340–350 | 92 | [270] |
| | potassium hydroxide | 340–350 | 94 | [270] |
| | sodium ethylate | 330–340 | 93 | [270] |
| | amalgam of alkaline metal | 310–320 | 90 | [270] |
| | sodium borohydride | 280–290 | 88 | [281] |
| | alkaline metal | 280–290 | 90 | [270] |
| HCOOK | no catalyst | 450–460 | 82 | [270] |
| | sodium hydroxide | 410–415 | 75 | [270] |
| | potassium hydroxide | 410–415 | 75 | [270] |
| | sodium amide | 180–200 | 85 | [268] [63] |
| | alkali hydride | 180–200 | 99 | [63] |
| | amalgam of alkaline metal | 200–210 | 90 | [270] |
| | alkaline metal | 180–190 | 96 | [270] |

kinetic values was different at the time and makes it hard to compare them to other studies. The reaction onset temperatures and oxalate yields, on the other hand, give a good indication of the activity of alkali metals. Pure metals showed exceptionally high selectivity towards oxalate with yields up to 94%. More importantly, the reaction temperature dropped significantly by 200 °C to the respective melting points of the formates. The major drawback of alkali metals is their high reactivity with water and oxygen.[291] They must be stored and processed in inert conditions, which makes it difficult and costly to utilize them on a large scale. Freidlin suggested using alkali amalgams to increase the metal's specific densities. The catalyst submerges in the reaction mass and has no contact with potential oxygen, whilst still being active. Then the amalgam could be recycled and put back in the reactor.[269] Although this makes catalyst recycling possible, today amalgams underlay strict restrictions as they pose health and environmental risks.[292] They also reported that sodium amide ($NaNH_2$) could potentially catalyze the reaction. They obtained 85% oxalate yield at 240 °C from potassium formate with 2–4 wt% loading of sodium amide. In our recent publication, we could show oxalate yields of 99% at 180 °C and loadings of 0.5 wt%. The disadvantage of using amide catalysts is the liberation of $NH_3$, which needs to be removed from the $H_2$ formed in the coupling reaction, while hydride catalysts just liberate $H_2$.[63]

Górski and Kraśnicka explored the addition of sodium borohydride ($NaBH_4$) to sodium formate.[279,282] The use of 5 mol% sodium borohydride at 290 °C leads to 88% oxalate yield from sodium formate, whilst with a 1:1 molar ratio no conversion was observed.

When ferric oxides are present on the reactor walls, the reaction is inhibited. If glass powder is added to the reaction, however, the yield increased up to 90%, which leads to the proposition of a chain mechanism where chain initiation might take place at a solid surface. This claim was not investigated further.[273]

The most recent additions are metal hydrides, which show similar base strength to alkaline metals but are easier to handle. They were first used by Lakkaraju et al., who reported a drop in reaction time and increase in yield but no drop in reaction temperature for sodium formate coupling.[34] Inspired by this, we tested various superbases as catalysts for the reaction. We found that absolute water- and oxygen-free reaction conditions are important. In these conditions, we observed for potassium formate coupling a reaction start corresponding to the melting of the substrate, reaction times of 30 s to 2 min, which is 10 times below the values reported by Lakkaraju et al., and yields between 97 and 99%.[63]

Hartman and Hisatsune estimated the activation energy of calcium formate decomposition in halide matrices using IR spectra. This led to an activation energy of $217.5 \pm 33.4\ kJ\,mol^{-1}$.[293] Lakkaraju et al. were yet the only ones who estimated the activation energy using a catalyst. They calculated an activation enthalpy of $171.5\ kJ\,mol^{-1}$ and activation entropy of $-25.1\ kJ^{-1}\,mol^{-1}$ for sodium formate coupling catalyzed by sodium hydride. These values account for an activation energy of approximately $177\ kJ\,mol^{-1}$ and a pre-exponential factor $A$ of $1.327 \times 10^{37}\ s^{-1}$. The high pre-exponential factor indicates mass transfer limitations in this case. We obtained $202\ kJ\,mol^{-1}$ for uncatalyzed reactions and $129\ kJ\,mol^{-1}$ for the KOH-catalyzed reaction with pre-exponential factors of $1.28 \times 10^{19}$ and $1.06 \times 10^{13}$, respectively, suggesting that physical effects such as mass transfer, substrate melting, or thermal loss due to gas formation only played a minor role in these reactions.[63]

This is however different for the newly proposed superbase catalysts, for which no sensible activation energies could be measured due to the coincidence of the reaction start with the physical phenomenon of substrate melting, which causes strong mass transfer effects.[63] The reaction then proceeds very vigorously due to the rapid availability of substrate for the reaction once it is molten. The real reaction start temperature thus cannot be investigated.

Over the years many different mechanisms were proposed for the seemingly simple coupling reaction.[34,278,280,283,293,294] These include studies on how alkali metals act in the reaction, the role of carbonite ion ($CO_2^{2-}$) as intermediate in the reaction, as well as on the gaseous products that are formed during formate decomposition. Górski and Kraśnicka were the first to suggest carbonite as an intermediate in the reaction in 1987.[280] In 2016, Lakkaraju et al. proposed a mechanism involving a hydride-catalyzed reaction including carbonite.[34] Carbonite dianions are strong nucleophiles and attack formate to form oxalate as shown in Scheme 9. In a recent Review, Paparo and Okuda discuss the reactivity and nature of the Carbonite species.[295]

The hydrogen atom from the attacked formate is released as a hydride, thereby regenerating the hydride catalyst. The postulated mechanism was supported with Raman measurements during the sodium formate coupling and density functional theory (DFT) calculations. In the DFT calculations, the respective energies of possible intermediates at different temperatures as shown in Figure 12 were calculated.

The rate-determining step (RDS) in the mechanism by Lakkaraju et al. is the deprotonation of formate by the catalyst. This is shown in Figure 12 as an $I_2 \rightarrow TS$ step, and the energy value for this step was estimated to be 41 kcal mol$^{-1}$. Although we were unable to observe the carbonite ion as intermediate in potassium formate coupling using in-situ Raman spectroscopy, we recently confirmed the involvement of carbonite intermediate by using isotope labeling in quenching studies.[63] Most recently, we reported the mechanism for the hydroxide-catalyzed reaction, which depends on the in-situ formation of the active hydride species and then follows the pathways described by Lakkaraju et al.[285]

In recent years the formate coupling reaction gained more commercial interest again with the upcoming CCU pathways

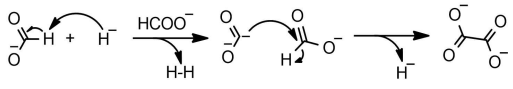


**Scheme 9.** Mechanism for hydride-catalyzed formate coupling reaction as postulated by Lakkaraju et al.[34]

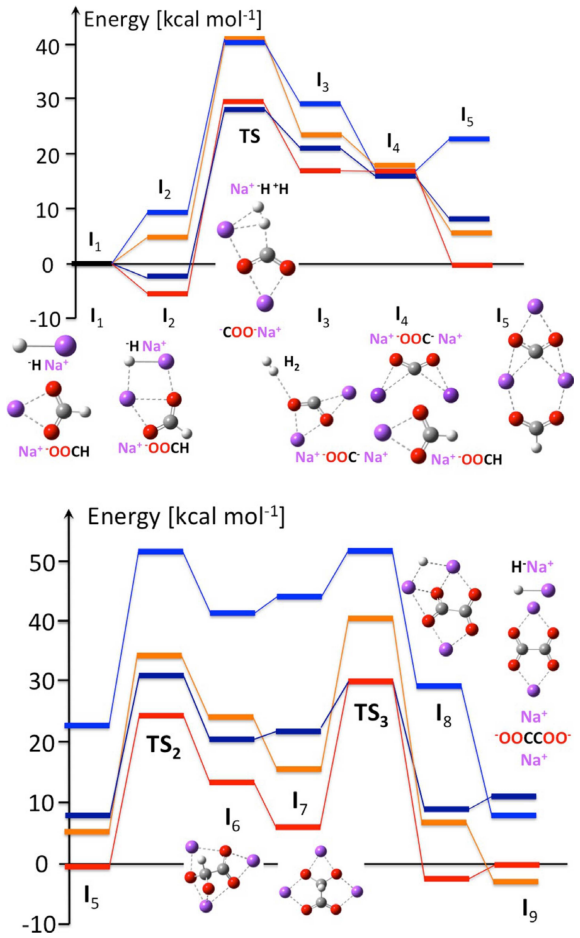


**Figure 12.** DFT free-energy calculations of the catalytic conversion of formate into oxalate as salts of sodium (red 663 K, orange 298 K) and potassium (navy 713 K, blue 298 K). Figure adapted with permission from Ref. [34]. Copyright 2016, Wiley-VCH.

including formate as intermediate. Several new patents and studies were published presenting new reactor designs for continuous operation. They often include advanced technologies such as microwave heating or the use of nozzles as used in spray dryers.[35,296–310] Overall, formate coupling provides a sustainable pathway to oxalate. The high yield is an advantage, and the previous drawbacks of high temperatures and long reaction times could recently be tackled with new catalyst types. Additionally, this reaction was performed for many decades on an industrial scale.

### 5.3. Acidification of oxalate to oxalic acid

In all previously described processes and the upcoming alkali fusion of biomass (Section 8.2), oxalate is produced. This requires the introduction of an acidification step to obtain oxalic acid. One option is the use of inorganic acids such as sulfuric or hydrochloric acid following Equation (36).[264]

$$(COOM)_2 + 2H^+ \rightarrow (COOH)_2 + 2M^+ \quad (36)$$

Electrodialysis is an alternative process that helps to avoid the use of corrosive acids and the formation of stoichiometric amounts of salts.[311–314] In an electrodialysis process, the alkali ion and the oxalate migrate to the cathode and anode, respectively, but the oxalate ions would be oxidized and decomposed by oxygen in the anodic compartment. To avoid this, cation and bipolar membranes are required. The simplest option is the use of two cation-exchange membranes as shown in Figure 13A. Protons are provided by water splitting in the hydrogen evolution reaction on the anode [Eq. (37)]. The hydroxy ions are provided by water splitting in the oxygen evolution reaction on the cathode [Eq. (38)].[312,315]

$$2\ H_2O \rightarrow 4\ e^- + 4\ H^+ + O_2 \quad (37)$$

$$4\ H_2O + 4\ e^- \rightarrow 4\ OH^- + 2\ H_2 \quad (38)$$

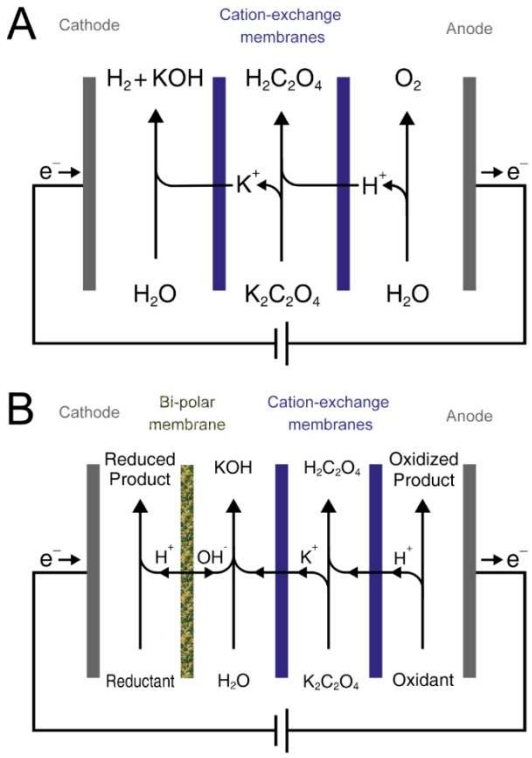


**Figure 13.** Simple electrolysis cell-design (A) uses two cation-exchange membranes (blue) to create three compartments. In the anodic compartment, the oxygen evolution reaction on the anode produces protons and oxygen. The protons migrate to the middle compartment, where they exchange potassium for a proton to form oxalic acid. The potassium migrates through the cation-exchange membrane to the cathodic compartment, where it forms potassium hydroxide with the hydroxide ions produced on the cathode during the hydrogen evolution reaction. In the advanced multifunctional cell (B), which has the fourth compartment by adding a bipolar membrane, the salt splitting can be coupled with the production of high-value chemicals. A reductant is reduced in the cathodic compartment and an oxidant is oxidized in the anodic compartment. The proton for the reduction is drawn from the bipolar membrane in which water splitting is taking place.

To improve the economic feasibility of the electrocatalytic salt splitting process it is desirable to produce high-value products with the invested electrons rather than perform water splitting. This can be achieved by combining the cation-exchange membrane with other membranes such as bipolar membranes.[316] In particular, electrodialysis bipolar membranes (EDBM) can be exploited for the production of organic acids via water splitting in bipolar membranes.[311]

EDBM can achieve the highest utilization of resources by supplying $H^+$ or $OH^-$ in situ and keeping the electrodes available to produce high-value products through oxidation and reduction reactions. The in-situ production has been successfully used for the production of formic acid, acetic acid, propionic acid, lactic acid, citric acid, gluconic acid, and many other carboxylic acids and amino acids.[314,315,317–320]

The concept of coupling with other reactions in a multi-compartment cell is shown in Figure 13B. Bipolar membranes are commercially available and are used in various processes such as desalination of industrial wastewater, lithium battery recycling, hydrochloric acid and sodium hydroxide production from brines, and magnesium recovery from seawater.[321–326] The coupling of the electrodialysis processes with other electrochemical reactions is still in development and requires more research to find reactions that can be coupled optimally in the separate compartments.

## 6. Ethylene Glycol Oxidation

Oxalic acid can be obtained from ethylene glycol (EG) via oxidation.[327–331] This route might be interesting in the future as new sustainable cost-competitive routes for EG production (e.g., from carbohydrates) emerge (Scheme 10).[102,332,333]

### 6.1. Ethylene glycol production

EG is a bulk chemical and commercially produced in megaton quantities mainly from fossil sources through ethylene oxide hydrolysis.[334] It is mainly used as a monomer for polyester (PET) production and as an anti-freeze agent and engine coolant additive. Alternative reaction pathways include coupling of CO and new pathways from biomass such as cellulose and glucose as well as from glycerol, which is produced on a large scale as a by-product in biodiesel refineries are developed and tested on a pilot scale.[333,335–339] Details of current EG production pathways and future development are described and discussed in great detail in various Reviews.[332,333,335,337,338] Overall, sustainable alternatives for the production of EG are available and increasingly employed on a commercial scale.

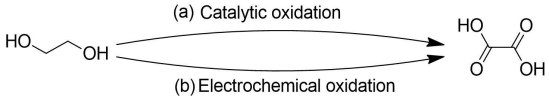


**Scheme 10.** (a) Ethylene glycol can be oxidized to oxalic acid by catalytic oxidation with oxygen or nitric acid. (b) A newer alternative route uses electrochemical oxidation.

### 6.2. Catalytic oxidation of ethylene glycol to oxalic acid

Oxalic acid production via EG oxidation is a simple one-step process as shown in Scheme 11 and was first patented by the Japanese company Mitsubishi in 1969.[327] Oxalic acid was produced at a high yield with the addition of an acid mixture comprising 2–60 wt% $HNO_3$, 20–78 wt% $H_2SO_4$, and 20–50 wt% $H_2O$. The molar ratio of $HNO_3$ to EG should not be less than 3:1.

The process has been further optimized by Mitsubishi with the introduction of gaseous oxygen, which oxidizes $NO_x$ gases generated in the process back to $HNO_3$ as shown in Scheme 12. An initiator, such as $NaNO_2$, may be used to generate nitrogen oxides, and a promoter, such as vanadium compounds or sulfuric acid, also may be employed to accelerate the oxidation reaction. The process eliminates the use of the $HNO_3$-regeneration system, which is required in the usual $HNO_3$ oxidation.[328] A further improvement was made by Ube Industries in Japan by operating only with nitric acid (no sulfuric acid) and $O_2$ as oxidant.

With this process, high yields of 95% based on EG can be achieved. The improved method is commercially used in Japan today and can also use propylene glycol, acetaldehyde, or glycolic acid as feedstock.[106]

### 6.3. Electrochemical oxidation of ethylene glycol to oxalic acid

Oxalic acid can also be electrochemically obtained from EG. This pathway became known during the search for alternatives to methanol as a fuel for direct oxidation fuel cells.[330] Oxalic acid is one of the possible oxidation products in fuel cell systems that are composed of $NaCo_2O_4$ and $LaSr_3Fe_3O_{10}$ electrolytes and Pt/C, PtRu/C, Pd/C, and Fe–Co–Ni/C anode catalysts.[329,340–342] EG can be electrochemically oxidized to oxalic acid with a reaction enthalpy $\Delta H_r$ of $-941\ kJ\,mol^{-1}$.[331] These fuel cells consequently generated a high output power density of $27\ mW\,cm^{-2}$ at a current density of $90\ mA\,cm^{-2}$.[331] The selective oxidation reaction proceeds ideally as follows [Eqs. (39–41)]:

$$\text{Anode}: (CH_2OH)_2 + 8\ OH^- \rightarrow (COOH)_2 + 6\ H_2O + 8\ e^- \quad (39)$$

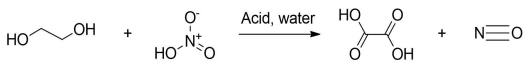


**Scheme 11.** Oxidation of ethylene glycol using mixed acids in water.

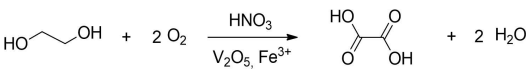


**Scheme 12.** Oxidation of ethylene glycol by nitric acid and oxygen.

$$\text{Cathode}: \ 2\ O_2 + 4\ H_2O + 8\ e^- \rightarrow 8\ OH^- \quad (40)$$

$$\text{Overall}: (CH_2OH)_2 + 2\ O_2 \rightarrow (COOH)_2 + 2\ H_2O \quad (41)$$

One of the main challenges is to suppress the cleavage of the C–C bond leading to $CO_2$ formation or oxidation towards glycolaldehyde, glycolic acid, glyoxal, formic acid, and $CO_2$.[329] Although this process is fairly well understood, no efforts have been made yet to use this process commercially.

## 7. Propylene or Ethylene Oxidation to Oxalic Acid

Oxalic acid can be obtained from propylene or ethylene via oxidation (Scheme 13). Propylene is an important chemical feedstock and is mostly known as a feedstock for polymers such as polypropylene or the production of acetonitrile and isopropanol.[343] Ethylene is one of the most common chemical building blocks and used in the production of polymers and intermediate chemical building blocks.[344]

### 7.1. Propylene and ethylene production

Commercially, propylene is solely produced from fossil sources including oil, natural gas, and coal. A shift in feedstock from oil to shale gas and coal has been seen in recent years. This changes propylene from being one of many products (cracking) to a targeted product in on-purpose processes.[345,346] On-purpose processes include propane dehydrogenation, acetic acid hydrogenation, olefin metathesis, and synthesis from methanol. These routes were described in detail by Zimmermann, Rodríguez-Vallejo et al., Kelly, and Torres Galvis and De Jong.[345–348] Similar to propylene, ethylene is mainly produced from fossil resources today. The main process is steam cracking of naphtha and ethane.[344,349] Other sources for ethylene include (chloro)methane, ethanol, syngas, or methanol.[344,350–352]

Alternatively, propylene can be obtained from renewable sources such as $CO_2$ and biomass mainly via the Fischer-Tropsch to Olefins process, the direct hydrogenation of $CO_2$ to light olefins, or dehydration of glucose-derived alcohols followed by metathesis as shown in Scheme 14.[348,353–357] There are multiple routes possible for the production of renewable ethylene. The production of bio-ethylene from bio-based ethanol is commercialized by a number of companies such as India glycols and Clariant.[352,358] A future potential route is from bio-methanol, the production of which is already commercialized.[359–362]

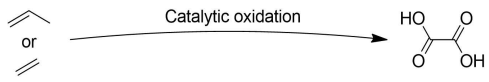


**Scheme 13.** Oxalic acid production from propylene or ethylene via catalytic oxidation.

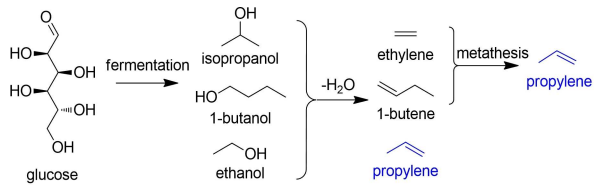


**Scheme 14.** Propylene production from glucose via fermentation, dehydration, and metathesis. Glucose is converted to alcohols including isopropanol, 1-butanol, and ethanol. The alcohols are co-dehydrated to the corresponding olefins, and 1-butene and ethylene are sent to a metathesis system to form more propylene.

### 7.2. Oxidation of propylene or ethylene to oxalic acid

Oxalic acid from the reaction of propylene with nitric acid is the second most important industrial process.[106] Originally developed in 1960 by Allied Corporation, oxalic acid is produced through the oxidation of propylene with mixed acids such as $HNO_3$, liquid $NO_2$, and $H_2SO_4$.[363] More specifically, propylene reacts with liquid $NO_2$ at −15 °C to form intermediate partial oxidation products. The partially oxidized products are then converted at 65–80 °C with mixed acid. Upon recrystallization of the crude product from water, at least 80% molar yield of pure oxalic acid can be obtained. Due to the use of $H_2SO_4$, severe equipment corrosion occurs during the process. The recovery of spent $H_2SO_4$ requires considerable water evaporation. Another drawback is that propylene does not react rapidly with mixed acid. This imposes process and equipment limitations but also introduces an element of hazard since unreacted propylene reacts with liberated $NO_2$ in the vapor space above the liquid level. These mixtures of olefins and $NO_2$ form extremely unstable explosive nitro-substances.[364]

Rhône-Poulenc, the largest oxalic acid producer in the world, improved the method and uses it exclusively.[106,365] In their method, the first reaction step can be operated at a temperature higher than 0 °C instead of −15 °C, and the second oxidation step is promoted by the use of oxygen instead of the corrosive sulfuric acid. These refinements increased the yield and solved serious safety problems. In the first step, propylene is mixed with $HNO_3$ at 10–40 °C and converted into α-nitratolactic acid and lactic acid. In the second step, α-nitratolactic acid is oxidized by oxygen in the presence of a catalyst at 45–100 °C to produce oxalic acid dihydrate as shown in Scheme 15.[366]

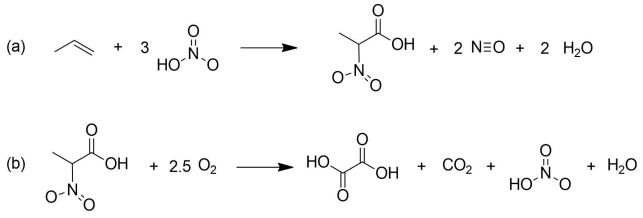


**Scheme 15.** Oxalic acid production from propylene starts with (a) propylene conversion to α-nitratolactic acid with nitric acid, followed by (b) oxidation by oxygen to oxalic acid.

The use of oxygen ensures both maximum oxidation and recovery of nitrous fumes ($NO_2 \rightleftarrows N_2O$, $N_2O_3$, and $HNO_2$), which are oxidized to nitric acid (used in first step). Nitrous fumes lead to degradation reactions. An improvement in the yield was achieved by the addition of catalysts (salts or compounds containing Fe, Al, Cr, Sn, Bi, or I).[366] The overall yield based on propylene is greater than 90%. Although this process has been used on a large commercial scale, it still suffers from safety problems because the nitrates of α-hydroxycarboxylic acids that are formed as intermediates from α-olefins and $NO_2$ are unstable and can lead to uncontrollable decomposition and explosions.[367] The production of $CO_2$ as a side product is a further drawback but can be overcome potentially by using ethylene instead of propylene in the process. Today both ethylene and propylene can be obtained from renewable sources, leading to a sustainable process. Especially bio-ethylene produced from bio-methanol or bio-ethanol is a promising substitute in this route as it avoids the production of $CO_2$ in the oxidation towards oxalic acid.[358]

The oxidation of propylene and especially ethylene is very interesting in terms of reaction mass efficiency. However, making them from oxygenated biomass requires the removal of oxygen first, followed by the addition of oxygen. This adds more complexity to the process, which may not be economically favorable.

## 8. Biomass to Oxalic Acid

Oxalic acid can be derived from biomass via three routes shown in Scheme 16. These include the oxidation of sugars, alkali heating of plant matter, or fermentation of sugars. In all cases, primarily the sugary contents of the plant matter either in the form of mono- or polysaccharides are converted to oxalic acid. Thus, it is important to use sugar-rich biomass such as sugarcane or sugar beets or high-cellulose tree varieties in these processes. Alternatively, biomass can serve as a source to produce most other substrates including $CO_2$, CO, EG, bio-propylene, or bio-ethylene. For sustainable production, second-, third-, and fourth-generation biomass should be used to avoid competition with food production. Similar to discussions about biofuels, the impact of fertilization, water, and land use for the production of biomass has to be considered too when comparing these processes.[168,368–373]

### 8.1. Oxidation of carbohydrates/biomass

The oldest method for the artificial production of oxalic acid with the use of nitric acid was first described by Bergmann in 1776.[37] This process was operated at a large scale in Bitterfeld, Germany until the 1990s and is still employed in Spain, Taiwan, Korea, India, Brazil, China, and several Eastern European countries.[106,374,375] Various kinds of biomass can be utilized as raw materials such as sucrose, cane molasses, gur, and cane juice.[79,81,92,93] In 1837, Barsham's invention introduced a new apparatus that keeps the harmful off-gases contained. This not only takes care of the factory building and its workers but also the neighbors who live close to the plants. The industry can also harness the entailed chemicals, improving the economics. The apparatus is a closed system for the production of oxalic acid from sugars and nitric acid.[80] The first optimized production process was introduced by Nyren in 1841. He used potatoes and chestnuts, which were first boiled to convert the starch to sugars, and subsequently sugars were transformed into oxalic acid by the addition of nitric acid.[376] Molasses and other agricultural waste can be used as an inexpensive raw material, which must be further processed in any case due to environmental reasons.[377,378] Depending on the starting materials, foam, greases, slime, and solids can form and require downstream separation. Non-optimal conditions drive the reaction to the formation of different side products, which further reduces the yield.[379]

A problem of the nitric acid oxidation of carbohydrates is the production of nitrogen oxides ($NO_x$), which have to be removed.[82] The oxidation may be enhanced using nitrogen dioxide ($NO_2$) instead of nitric acid. Nitrogen dioxide has been recommended as an inexpensive oxidizing agent for the production of oxalic acid from carbohydrates.[86] Alternatively, the oxidation can be carried out with aqueous nitric acid of at least 50% concentration by weight at a temperature of 40–120 °C.[78]

A process developed by Allied Chemical corporation as shown in Scheme 17 uses glucose solution obtained from hydrolyzed starch, which is converted with nitric and sulfuric acid in the presence of vanadium pentoxide and iron(III) sulfate as a catalyst.[76,380,381] Overall, this process is highly exothermic and requires cooling as it is sensitive to temperature. Thus a controlled range between 65–70 °C is required to avoid side reactions.[381] The $NO_x$ gases are recovered by absorption in water or weak nitric acid in the presence of free oxygen under elevated pressure. Independent work on the process concluded that air flow rate, temperature, the amount of $V_2O_5$ catalyst, and concentrations of glucose, $H_2SO_4$, and $HNO_3$ all strongly affect the yields.[82] 65% of the introduced carbon from sugar is

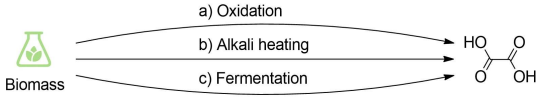


**Scheme 16.** Oxalic acid can be obtained from biomass via (a) oxidation, (b) alkali heating, and (c) fermentation.

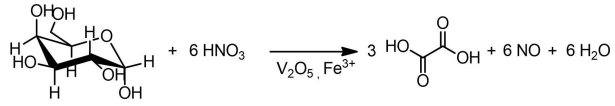


**Scheme 17.** Oxidation of glucose to oxalic acid with nitric acid, catalyzed by vanadium pentoxide.

converted to oxalic acid while 35% is lost to $CO_2$ as a side product.[380]

### 8.2. Alkali fusion of biomass

In 1829, Gay-Lussac proposed the heating of carbohydrates and later of wood with sodium or potassium hydroxide at 240–285 °C to produce oxalic acid.[77,250] Scheme 18 illustrates the oxalic acid production process in which the biomass is heated with an alkali solution to yield sodium or potassium oxalate. This is then precipitated as magnesium oxalate with the addition of magnesium chloride, from which oxalic acid is obtained by acidification with a strong acid.

Thorn studied the manufacturing of oxalic acid from sawdust of various wood varieties heated with KOH and obtained an 80% carbon yield of oxalic acid.[382] The oxalic acid is decomposed if a critical reaction mass is exceeded. This was attributed to the excess heat of the system coming from the exothermicity of the reaction.[87] The mixture should be heated in thin layers.[85] Since NaOH is cheaper it is preferred to KOH, but using only NaOH leads to significantly lower yields compared to KOH. Roberts et al. recognized that a mixture of NaOH and KOH could be used and patented the production of oxalic acid from sawdust using a mixture of NaOH and KOH.[94] They found that the optimal mixing ratio of NaOH to KOH is 2:3. Thorn's experiments confirmed this ratio as it offered a yield almost as good as with pure KOH when heated in thin layers, but using less than 40% KOH reduced the yield drastically. The required concentration of the lye was found to be 10–15 mol $L^{-1}$.[85]

For the reaction, 40 wt% sawdust is added to the alkaline solution. This mix is heated above 200 °C, and the oxalate can be purified by adding water to remove the alkali and residual sugars. A total of 17 potential feedstocks were tested by Possoz, and wheat spelt as well as tobacco ribs were the most promising reported.[383]

In 1923, Alcock proposed an alternative oxalic acid recovery where sulfuric acid is added to the dissolved oxalate to convert the oxalate to oxalic acid, which was hot-filtered to remove solid residues. Due to its low solubility, oxalic acid precipitates during cooling and can be removed from the solution.[73]

There are several limitations to this process, such as the use of thin layers to avoid the fusion of mass. Moreover, an increase in the proportion of sawdust to the alkali causes practical difficulties in heating the mass and in subsequent extraction of the acid. After the synthesis of oxalate, more chemicals such as corrosive acids and time-consuming steps are needed to obtain the final product in pure form.[90] This method has now been replaced by more up-to-date methods.[77]

### 8.3. Fermentation of carbohydrates

Oxalic acid was first discovered in clover (*oxalis*), and hence plants can be used as molecular factories to produce it (Scheme 19).[37] Various lower forms of plants can produce the acid from carbohydrate food sources, but its extraction is not commercially viable. However, also some fungi from the family of *trichocomaceae*, including *aspergillum* or *penicillium*, produce oxalic acid with their oxaloacetate hydrolase, and *aspergillus niger* is considered the best out of those.[69,70,72]

However, the fungi do not purely produce oxalic acid but a mix of citric, oxalic, and gluconic acid.[69] Oxalic acid is a side product in this process but can be promoted by performing the reaction in slightly acidic or neutral media.[71] The fungi produce oxalic acid as an acid regulator to prevent competitive organisms' growth.[68]

Strasser et al. and Cameselle et al. established sucrose and lactose as the ideal carbon and energy source to produce oxalic acid at a pH higher than 6.[69,99,100] Glucose is not considered a good feedstock as it is primarily is converted to gluconic acid.[69]

To reach economic high yields in oxalate, the fermentation of low-cost carbon substrates, namely carbon waste streams, is ideal. Strasser et al. established that green syrup, lactose permeate, and molasses are suitable substrates, and they could reach 80% conversion and 38.7% oxalic acid selectivity.[69] Recent research has seen this number increase to 58.8%, which still requires separation of oxalic acid from the cell media and gluconic acid by-product.[74,97]

## 9. Comparison

With so many potential pathways available to produce oxalic acid, there is hardly only one perfect solution. This is also evident from the many different processes and feedstocks that have been used in the past. However, the new challenges to produce chemicals in a green or better circular way pose a different set of requirements to these processes. To achieve an overall sustainable process two strategies are available: the development and upscaling of new routes or the retrofitting of existing processes mainly in the feedstock sourcing section.

We evaluate each of the process steps on their sustainability using the 12 green chemistry principles.[384] Overall, we use 8 categories that include: feedstock source, process toxicity, waste

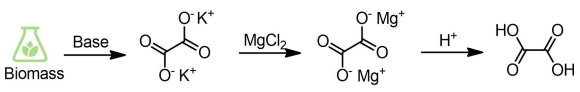


**Scheme 18.** Alkali fusion process to obtain oxalic acid from biomass. Steps include the heating of biomass with alkali solution, magnesium oxalate precipitation, and finally acidification.

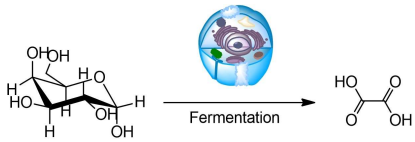


**Scheme 19.** Fermentation of sugars to oxalic acid.

production, use of precious materials, energy source, the harshness of process conditions, and need for downstream separation. In addition, we calculated the atom economy and reaction mass efficiency (RME) based on the best-of-class reported yields. For all the subcategories, a rating on a 5-star scale is used, where 5 stars stand for the highest sustainability. A comprehensive overview of the rating is presented in Table 4, and Figure 14 provides an overview of all routes including their sustainability and maturity.

Direct $CO_2$ reduction, alkali fusion of biomass, and formate-based processes produce oxalate as an intermediate. The most advanced option is the zinc-oxalate process, but it lacks proof of principle on the pilot stage and requires organic solvents with highly water-free environments. New water-based or water-tolerant processes are now emerging but are at a very early stage of development still. Metal-complex catalysts deliver high yields and work with abundant metals. However, they require complex catalyst structures, dry organic solvents, and have not yet been demonstrated in a continuous process. The last alternative for direct conversion suggests the use of AA (Vitamin C) to capture and transform $CO_2$ to oxalate. The AA is consumed in the process, which is reflected in the low atom economy of this process. Additionally, AA production requires multiple steps and is expensive, and therefore this option seems not suitable.

Alkali fusion of biomass is one of the oldest production methods for oxalate and oxalic acid but suffers from low yields and has the lowest atom economy and RME of all processes. The resulting complex product mixtures require intensive separation steps.

Indirect pathways to produce oxalate use formate as feedstock. Formate can be sustainably produced from $CO_2$ via five

**Table 4.** Comparison and evaluation of all routes and sub-routes based on atom economy, RME, sustainability based on green chemistry principles, and maturity.

| Primary pathway | Process step | Atom economy[a] [%] | RME[b] [%] | Sustainability[c] (1–5) | Maturity[d] |
|---|---|---|---|---|---|
| direct conversion of $CO_2$ | classic electrochemistry | 152 | 137 | 3.50 | bench |
| | metal-complex electrochemistry | 152 | 146 | 3.65 | lab |
| | sacrificial ascorbate reduction | 61 | 49 | 3.93 | lab |
| formate coupling | carbonate reduction | 79 | 78 | 4.21 | bench |
| | photochemical reduction | 73 | 69 | 4.21 | pilot |
| | photochemical reduction | 73 | 47 | 3.87 | bench |
| | enzymatic production | – | – | 4.14 | bench |
| | caustic CO reduction | 100 | 97 | 3.93 | commercial |
| | formate coupling | 99 | 98 | 4.36 | commercial |
| CO to oxalic acid | Boudouard reaction | 100 | 80 | 2.00 | commercial |
| | coal gasification | 33 | 8 | 3.29 | commercial |
| | steam reforming | 93 | 75 | 1.86 | commercial |
| | partial oxidation | 92 | 74 | 2.21 | commercial |
| | biomass gasification | X | X | 4.14 | pilot |
| | reverse water-gas shift | 61 | 33 | 4.14 | commercial |
| | electrochemical reduction | 61 | 52 | 4.07 | bench |
| | photochemical reduction | 61 | 61 | 4.14 | lab |
| | electrolysis (solid oxide electrolyzer cell) | 64 | 51 | 4.14 | commercial |
| | dialkyl oxalate process | 98 | 96 | 3.00 | commercial |
| direct biomass conversion | alkali fusion | 27 | 22 | 2.79 | commercial |
| | oxidation | 92 | 60 | 3.79 | commercial |
| | fermentation | X | X | 3.86 | bench |
| EG oxidation | ethylene oxide hydrolysis | 100 | 90 | 1.96 | commercial |
| | glycerol oxidation | 69 | 59 | 3.93 | pilot |
| | catalytic EG oxidation | 71 | 67 | 3.71 | commercial |
| | electrochemical EG oxidation | 71 | 67 | 4.22 | bench |
| propylene oxidation | steam cracking | 90 | 90 | 1.93 | commercial |
| | fossil on-purpose processes | X | X | 1.85 | commercial |
| | bioethanol dehydrogenation | 53 | 48 | 3.14 | pilot |
| | Fischer-Tropsch to olefins | 67 | 64 | 3.12 | lab |
| | direct hydrogenation | 36 | 33 | 3.21 | lab |
| | catalytic propylene oxidation | 32 | 36 | 3.07 | commercial |
| oxalate acidification | classic acidification | 44 | 44 | 4.29 | commercial |
| | paired electrodialysis | 85 | 84 | 4.71 | bench |

X = could not be calculated. [a] Atom economy = (mass of all products/mass of all reactants) × 100. [b] Reaction mass efficiency = actual yield of all process steps combined × (mass of all products)/(mass of all reactants). [c] Sustainability rating is a rating on the overall sustainability of the process on a 1–5 scale, where 1 is the worst and 5 is the best achievable rating. The rating considers seven categories for which different impacts were attributed and are listed with descending impact: feedstock sustainability (Impact: 5), production of waste and greenhouse gases (Impact: 3), use of precious materials or solvents (Impact: 2), energy source process toxicity and safety concerns (Impact: 2), intensity of downstream separation (Impact: 1), energy efficiency and process conditions (Impact: 1). For all sub-categories, a rating from 1 (worst) to 5 (best) was given. The overall rating reflects the average of the sum of grades for all categories weighted by their impact factors. [d] Maturity reflects scale at which a process is proven: lab-scale includes non-automized or optimized systems at low or sub gram scale (TRL 1–2); bench-scale includes processes that are performed at a high g or kg scale with upscaling and optimization in mind (TRL 3–5); pilot-scale includes processes that are performed at a large kg or low ton scale to demonstrate the process (TRL 5–7); commercial-scale includes processes that have been used successfully commercially.

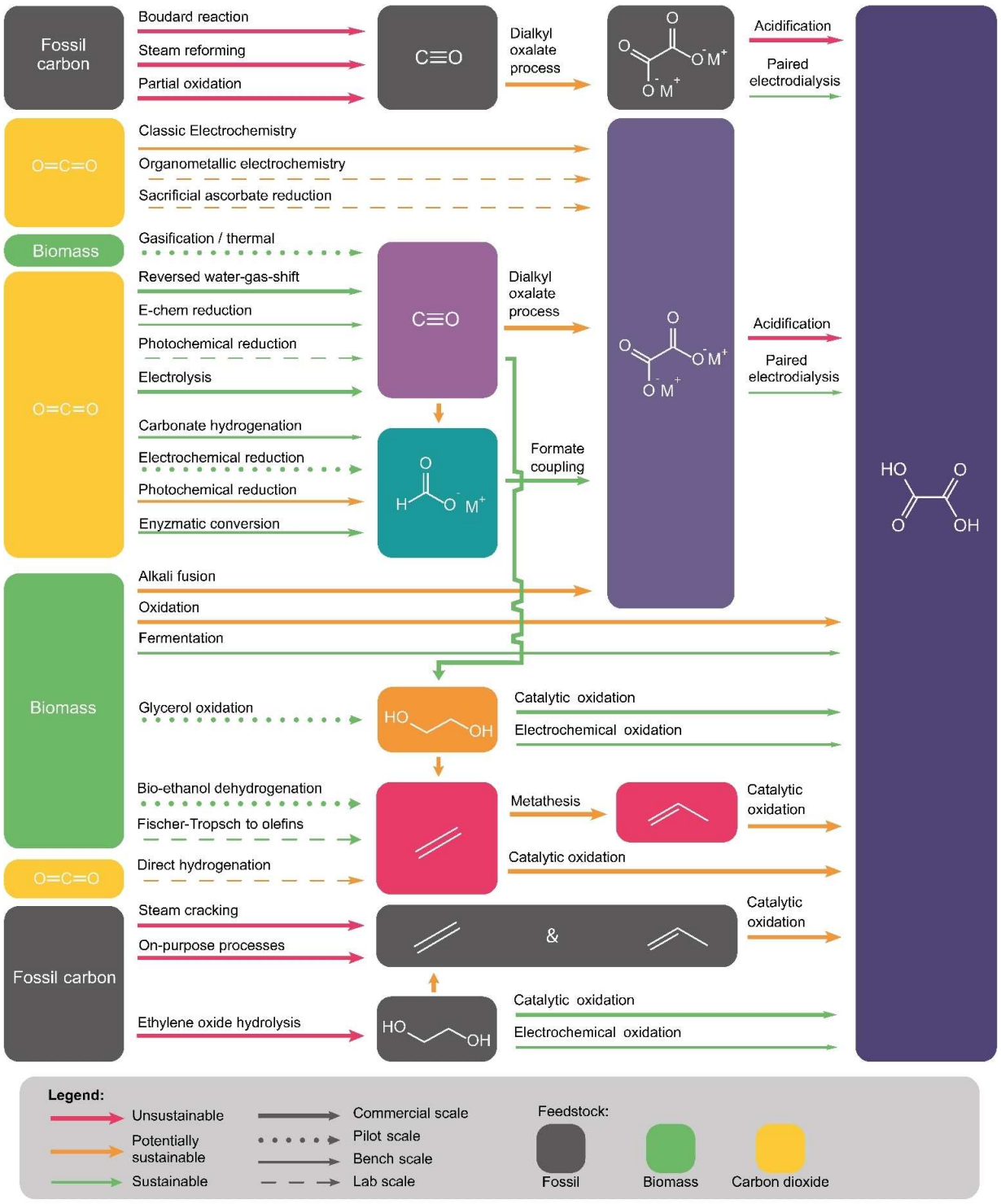


**Figure 14.** Overview of all potential routes that connect the three feedstocks (slate: fossil; green: biomass; yellow: $CO_2$) with the product side. All processes are graded on their sustainability in a three-color scheme. The colors are based on the grading as in Table 4 (red: < 2; yellow: < 4, green: > 4) The arrow style indicates the maturity of the process. Fossil pathways were kept separate from biomass and $CO_2$ pathways.

different pathways. Commercially, formate is produced from CO and caustic, but this has the drawback of consuming stoichiometric amounts of the base. The electrochemical reduction in aqueous systems has advanced rapidly in recent years, and the first pilot systems are tested now. In the future, photocatalytic or enzymatic processes might become relevant but are still at a very early stage today. The conversion to oxalic acid via simple acidification is not sustainable due to the use of stoichiometric amounts of strong acids. Paired electrodialysis, potentially even in multicompetent cells, is a promising alternative and can

couple the acidification step with other steps in the oxalic acid production, such as the production of base needed for formate production.

The direct conversion of carbohydrate-rich biomass to oxalic acid via oxidation was a widely used commercial process. It is, however, not very sustainable due to its low yields, use of corrosive acids, production of $CO_2$ as a by-product, and dependency on food-competitive feedstock such as glucose. An alternative is the fermentation of sugar-rich carbon waste streams with fungi. Although this improves the sustainability on the feedstock side, the process results in a product mixture that requires tedious separation and makes atom economy calculations impossible.

Today, the four main resources for oxalic acid production are CO in the dialkyl oxalate process, $CO_2$, carbohydrates including EG, and hydrocarbons such as ethylene or propylene, which are converted by catalytic oxidations.[106] Those feedstocks are either derived from fossil sources or bio-based. Although starch-based processes are not competing with food today, we need to make sure that in the long term, when bio-based production volumes may become very large, non-food biomass residues (second-generation biomass) are used as feedstock. Some of those processes, however, can also be performed with more sustainable feedstock.

Many sustainable options for CO generation are available, including electrolysis and reverse water-gas shift. Their low atom economy and RME numbers stem from the production of oxygen as a low-value side product. Carbon used in steam reforming or Boudouard reactions could also be sourced from waste streams. CO is converted via the commercially used dialkyl oxalate process, which is highly efficient in terms of atom efficiency and RME but requires the use of precious palladium as a catalyst and large amounts of dehydrating agents.

Sustainable CO is also already used as an alternative source to produce EG to replace the fossil-based ethylene oxide process. Another alternative to fossil-based EG is the oxidation of the waste stream glycerol from biomass, which is already tested on a pilot scale. The subsequent oxidation of EG is a sustainable process that uses non-precious catalysts and oxygen from the air. Alternatively, the oxidation can be performed electrochemically. This process can be performed with non-precious metals as catalysts and has the added benefit of producing surplus energy. This would potentially allow coupling with the reduction of $CO_2$ in the other half-cell of an electrochemical process and reduce overall power cost.

Propylene or ethylene can be oxidized to oxalic acid with nitric acid. Extensive temperature control, safety problems, and the formation of $CO_2$ are problems in terms of sustainability in this process. The production of propylene itself is currently mainly fossil-based. Sustainable alternatives are tested in pilot plants. However, propylene is a viable chemical itself, and its production from biomass or $CO_2$ is achieved by an energy-intensive reduction reaction. It is questionable from a sustainability perspective to produce oxalic acid in a process that requires multiple energy-intensive steps.

## 10. Conclusion and Outlook

Overall, there are many pathways in the development for sustainable production of oxalic acid with the possibility of tapping into diverse feedstock options, including $CO_2$ and biomass. Many of the electrochemical routes additionally allow the use of renewable energy flexibly and therefore contribute solutions to the intermittency problem of renewable energy. Sustainable options closest to market introduction are production via CO from reverse water-gas shift or electrolysis using $CO_2$ as a feedstock in the dialkyl process. Some sustainable processes utilize waste streams, which limits their scalability to the availability and scale of the waste stream.

Our evaluation shows that the most sustainable routes to oxalic acid all start with $CO_2$ or biomass waste streams. The electrocatalytic or photocatalytic production of formate followed by formate coupling and paired electrodialysis is one of the contenders for the most sustainable option. Alternatives are provided by CO-based processes, where CO is produced from $CO_2$ either by reverse water-gas shift, solid oxide electrolyzer cell electrolysis, or by electrochemical reduction. Especially the coupling of CO to ethylene glycol followed by electrochemical oxidation is interesting as the two electrochemical steps can potentially be integrated.

There is still a long way ahead towards new sustainable processes to produce oxalic acid to the market. We recognize that many of the processes are at an early or at least very different development stages. This poses problems to the integration of the processes and techno-economic analysis of the processes. In programs such as the OCEAN, we try to integrate the subsequent steps with an open eye on alternatives. We need more economic and social incentives to encourage the development and integration of new routes towards sustainable oxalic acid and to unlock its potential as an economically attractive new platform chemical.

## *Acknowledgements*

*This project has received funding from the European Union's Horizon 2020 Research and Innovation Program under Grant Agreement No. 767798.*

## *Conflict of Interest*

The authors declare no conflict of interest.

**Keywords:** carbon capture and utilization · catalysis · $CO_2$ conversion · formate coupling · oxalic acid

[1] C. Levett, D. Carrington, "The climate crisis explained in 10 charts," can be found under https://www.theguardian.com/environment/2019/sep/20/the-climate-crisis-explained-in-10-charts, **2019**.
[2] J. Watts, "Human society under urgent threat from loss of Earth's natural life," can be found under https://www.theguardian.com/

environment/2019/may/06/human-society-under-urgent-threat-loss-earth-natural-life-un-report, **2019**.
[3] A. Leonard, "Our plastic pollution crisis is too big for recycling to fix," can be found under https://www.theguardian.com/commentisfree/2018/jun/09/recycling-plastic-crisis-oceans-pollution-corporate-responsibility, **2018**.
[4] M. K. Van Aalst, *Disasters* **2006**, *30*, 5–18.
[5] R. K. Pachauri, L. Meyer, Climate Change 2014: Synthesis Report. Contribution of Working Groups I, II and III to the Fifth Assessment Report of the Intergovernmental Panel on Climate Change, Gian-Kasper Plattner, Geneva, **2014**.
[6] E. Dlugokencky, P. Tans, *Trends in Atmospheric Carbon Dioxide*, can be found under https://www.esrl.noaa.gov/gmd/webdata/ccgg/trends/co2/co2_annmean_gl.txt, **2021**.
[7] P. Friedlingstein, M. O'Sullivan, M. W. Jones, R. M. Andrew, J. Hauck, A. Olsen, G. P. Peters, W. Peters, J. Pongratz, S. Sitch, C. Le Quéré, J. G. Canadell, P. Ciais, R. B. Jackson, S. Alin, et al., *Earth Syst. Sci. Data* **2020**, *12*, 3269–3340.
[8] C. Quéré, R. M. Andrew, P. Friedlingstein, S. Sitch, J. Hauck, J. Pongratz, P. A. Pickers, J. Ivar Korsbakken, G. P. Peters, J. G. Canadell, A. Arneth, V. K. Arora, L. Barbero, A. Bastos, L. Bopp, et al., *Earth Syst. Sci. Data* **2018**, *10*, 2141–2194.
[9] P. Styring, E. A. Quadrelli, K. Armstrong in *Carbon Dioxide Util. Closing Carbon Cycle, 1st ed.*, Elsevier, **2015**, pp. 237–272.
[10] J. Bollen in *Designing Sustainable Technologies, Products and Policies*, Springer International Publishing, Cham, **2018**, pp. 307–309.
[11] M. Aresta in *An Economy Based on Carbon Dioxide and Water*, Springer International Publishing, Cham, **2019**, pp. 431–436.
[12] F. D. Meylan, V. Moreau, S. Erkman, *J. $CO_2$ Util.* **2015**, *12*, 101–108.
[13] International energy agency, *Putting $CO_2$ to Use*, OECD, Paris, **2019**.
[14] W. Steffen, K. Richardson, J. Rockstrom, S. E. Cornell, I. Fetzer, E. M. Bennett, R. Biggs, S. R. Carpenter, W. de Vries, C. A. de Wit, C. Folke, D. Gerten, J. Heinke, G. M. Mace, L. M. Persson, V. Ramanathan, B. Reyers, S. Sorlin, *Science* **2015**, *347*, 1259855–1259855.
[15] B. Janusz, P. Dykstra, E. Fortunato, R.-D. Heuer, C. Keskitalo, P. Nurse, *Novel Carbon Capture and Utilisation Technologies (Brussels)* **2018**.
[16] Shell International B. V., "Shell Scenarios: Sky – Meeting the goals of The Paris agreement," **2018**.
[17] P. G. Levi, J. M. Cullen, *Environ. Sci. Technol.* **2018**, *52*, 1725–1734.
[18] I. A. G. Wilson, P. Styring, *Front. Energy Res.* **2017**, *5*, 1–10.
[19] T. Keijer, V. Bakker, J. C. Slootweg, *Nat. Chem.* **2019**, *11*, 190–195.
[20] C. Ampelli, S. Perathoner, G. Centi, *Philos. Trans. R. Soc. London* **2015**, *373*, 20140177.
[21] A. Kätelhön, R. Meys, S. Deutz, S. Suh, A. Bardow, *Proc. Natl. Acad. Sci. USA* **2019**, *166*, 11187–11194.
[22] J. Bujnicki, P. Dykstra, E. Fortunato, R.-D. Heuer, C. Keskitalo, P. Nurse, Group of Chief Scientific Advisors Scientific Opinion: Novel Carbon Capture and Utilisation Technologies, Brussels, **2018**.
[23] J. Schneider, H. Jia, J. T. Muckerman, E. Fujita, *Chem. Soc. Rev.* **2012**, *41*, 2036–2051.
[24] D. T. Whipple, P. J. A. Kenis, *J. Phys. Chem. Lett.* **2010**, *1*, 3451–3458.
[25] K. Li, X. An, K. H. Park, M. Khraisheh, J. Tang, *Catal. Today* **2014**, *224*, 3–12.
[26] P. De Luna, C. Hahn, D. Higgins, S. A. Jaffer, T. F. Jaramillo, E. H. Sargent, *Science* **2019**, *364*, eaav3506.
[27] J. Artz, T. E. Müller, K. Thenert, J. Kleinekorte, R. Meys, A. Sternberg, A. Bardow, W. Leitner, *Chem. Rev.* **2018**, *118*, 434–504.
[28] M. S. Reisch, *Chem. Eng. News* **2015**, *93*, 15.
[29] D. Derbyshire, "Liquid Light finds use for polluting CO2 gas," can be found under https://www.theguardian.com/technology/2014/dec/08/liquid-light-co2-greenhouse-gas-plastics-pet, **2014**.
[30] J. J. Kaczur, T. J. Kramer, K. Keyshar, P. Majsztrik, Z. Twardowski, Avantium Knowledge Centre B.V; US2013180863 A1, **2013**.
[31] J. J. Kaczur, T. J. Kramer, K. Keyshar, P. Majsztrik, Z. Twardowski, Avantium Knowledge Centre B.V; US2013180863A1, **2012**.
[32] J. J. Kaczur, P. Lakkaraju, K. Teamey, Avantium Knowledge Centre B.V, US10329676B2, **2015**.
[33] M. F. Philips, G. J. M. Gruter, M. T. M. Koper, K. J. P. Schouten, *ACS Sustainable Chem. Eng.* **2020**, *8*, 15430–15444.
[34] P. S. Lakkaraju, M. Askerka, H. Beyer, C. T. Ryan, T. Dobbins, C. Bennett, J. J. Kaczur, V. S. Batista, *ChemCatChem* **2016**, *8*, 3453–3457.
[35] J. J. Kaczur, P. P. Lakkaraju, R. R. Parajuli, Avantium Knowledge Centre B.V., WO2017121887A1, **2017**.
[36] "Oxalic acid from CO2 using Eletrochemistry At demonstratioN scale | OCEAN Project | H2020 | CORDIS | European Commission," can be found under https://cordis.europa.eu/project/id/767798, **2020**.
[37] Wöhler, *Polytech. J.* **1824**, *15*, 177–184.
[38] F. Abraham, B. Arab-Chapelet, M. Rivenet, C. Tamain, S. Grandjean, *Coord. Chem. Rev.* **2014**, *266–267*, 28–68.
[39] C. Kundu, H. J. Lee, J. W. Lee, *Bioresour. Technol.* **2015**, *178*, 28–35.
[40] D. Lesmana, H. S. Wu, *Energy* **2014**, *69*, 769–777.
[41] A. Augustyn, A. Gaur, G. Lotha, S. Singh, *Encyclopedia Britannica*, 19 Dec. 2018, can be found under: https://www.britannica.com/science/oxalic-acid, accessed 12 August 2021.
[42] N. B. Horeh, S. M. Mousavi, S. A. Shojaosadati, *J. Power Sources* **2016**, *320*, 257–266.
[43] Z. Wang, J. Cao, W. Jiang, *Postharvest Biol. Technol.* **2016**, *114*, 10–16.
[44] G. Centi, G. Iaquaniello, S. Perathoner, *BMC Chem. Eng.* **2019**, *1*, 5.
[45] S. Perathoner, G. Centi, *Catal. Today* **2019**, *330*, 157–170.
[46] M. A. Murcia Valderrama, R.-J. van Putten, G.-J. M. Gruter, *Eur. Polym. J.* **2019**, *119*, 445–468.
[47] M. A. Murcia Valderrama, R.-J. van Putten, G.-J. M. Gruter, *ACS Appl. Polym. Mater.* **2020**, *2*, 2706–2718.
[48] J. Nayler, H. Smith, Beecham Research Laboratories Ltd GB978178A, **1962**.
[49] W. Qin, Y. Zhang, Z. Li, Y. Dai, *J. Chem. Eng. Data* **2003**, *48*, 430–434.
[50] J.-C. Vallejos, Y. Christidis, Sanofi Aventis France, FR2470127 A1, **1979**.
[51] J. E. Seip, S. K. Fager, J. E. Gavagan, L. W. Gosser, D. L. Anton, R. DiCosimo, *J. Org. Chem.* **1993**, *58*, 2253–2259.
[52] S. Fredenberg, M. Wahlgren, M. Reslow, A. Axelsson, *Int. J. Pharm.* **2011**, *415*, 34–52.
[53] R. DiCosimo, M. S. Payne, A. Panova, J. Thompson, D. P. O'Keefe,Chemours Co FC LLC; US7198927B2, **2007**.
[54] O. M. Koivistoinen, J. Kuivanen, D. Barth, H. Turkia, J. P. Pitkänen, M. Penttilä, P. Richard, *Microb. Cell Fact.* **2013**, *12*, 1–16.
[55] B. Pereira, Z. J. Li, M. De Mey, C. G. Lim, H. Zhang, C. Hoeltgen, G. Stephanopoulos, *Metab. Eng.* **2016**, *34*, 80–87.
[56] S. Yunhai, S. Houyong, L. Deming, L. Qinghua, C. Dexing, Z. Yongchuan, *Sep. Purif. Technol.* **2006**, *49*, 20–26.
[57] G. Mattioda, Y. Christidis in *Ullmann's Encyclopedia of Industrial Chemistry*, Wiley-VCH, Weinheim, **2000**, pp. 89–92.
[58] W. Faveere, T. Mihaylov, M. Pelckmans, K. Moonen, F. Gillis-D'Hamers, R. Bosschaerts, K. Pierloot, B. F. Sels, *ACS Catal.* **2020**, *10*, 391–404.
[59] J. Xu, W. Huang, R. Bai, Y. Queneau, F. Jérôme, Y. Gu, *Green Chem.* **2019**, *21*, 2061–2069.
[60] F. Kawai, *Biopolym. Online* **2005**, DOI: 10.1002/3527600035.bpol9012.
[61] M. Crutchfield, V. Papanu, C. Warren, Solutia Inc.,US4144226, **1979**.
[62] E. Palm, L. J. Nilsson, M. Åhman, *J. Cleaner Prod.* **2016**, *129*, 548–555.
[63] E. Schuler, P. A. Ermolich, R. N. Shiju, G.-J. M. Gruter, *ChemSusChem* **2021**, *14*, 1517–1523.
[64] C. L. Beadle, S. P. Long, *Biomass* **1985**, *8*, 119–168.
[65] S. Prasad, A. P. Ingle in *Sustainable Bioenergy*, Elsevier, **2019**, pp. 327–346.
[66] A. Muscat, E. M. de Olde, I. J. M. de Boer, R. Ripoll-Bosch, *Glob. Food Sec.* 25, **2019**, DOI:10.1016/j.gfs.2019.100330
[67] N. A. Cashen, R. M. H. Kullman, R. M. Reinhardt, US Department of Agriculture USDA, US3811210, **1972**.
[68] L. Poulsen, M. R. Andersen, A. E. Lantz, J. Thykaer, *PLoS One* **2012**, *7*, e50596.
[69] H. Strasser, W. Burgstaller, F. Schinner, *FEMS Microbiol. Lett.* **1994**, *119*, 365–370.
[70] W. Podgorski, W. Lesniak in *Chemical Papers*, **2003**, pp. 408–412.
[71] M. Papagianni, *Biotechnol. Adv.* **2007**, *25*, 244–263.
[72] I. Musial, W. Rymowicz, D. Witkowska, *Chem. Pap.* **2006**, *60*, 388–390.
[73] J. R. Alcock A Method for the Preparation of Oxalic Acid From Sawdust, Bachelor Thesis **1923**, 12, DOI:10.7907/256R-2144.
[74] E. Walaszczyk, W. Podgórski, M. Janczar-Smuga, E. Dymarska, *Chem. Pap.* **2018**, *72*, 1089–1093.
[75] L. A. Possoz, *Polytech. J.* **1859**, *154*, 60–62.
[76] G. S. Simpson, General Chemical Corp, US2057119 A, **1933**.
[77] R. H. Farmer, in *Chem. Util. Wood*, Elsevier, **1967**, pp. 87–88.
[78] J. M. L. M. Elie, M. Duroux, L. M. Duroux, Rhone Poulenc SA, US3549696A, **1967**.
[79] A. C. Raha, R. B. Nigam, P. Sanyal, in *Proc. Annu. Conv. STAI*, **1976**, pp. 1–6.
[80] Barsham, *Polytech. J.* **1837**, *63*, 455–457.
[81] S. D. Deshpande, S. N. Vyas, *Ind. Eng. Chem. Prod. Res. Dev.* **1979**, *18*, 69–71.

[82] M. Gürü, A. Y. Bilgesü, V. Pamuk, *Bioresour. Technol.* **2001**, *77*, 81–86.
[83] E. Sarka, Z. Bubnik, A. Hinkova, J. Gebler, P. Kadlec, *Procedia Eng.* **2012**, *42*, 1219–1228.
[84] L. Possoz, *Polytech. J.* **1858**, *150*, 382–383.
[85] W. Thorn, *Polytech. J.* **1873**, *210*, 24–39.
[86] O. Varela in *Advances in Carbohydrate Chemistry and Biochemistry*, **2003**, pp. 307–369.
[87] L. Possoz, *Polytech. J.* **1858**, *150*, 127–130.
[88] G. Simpson, General Chemical Corp, US2057119 A, **1936**.
[89] P. Li, F. Yin, L. Song, X. Zheng, *Food Chem.* **2016**, *202*, 125–132.
[90] W.Thorn, The London, Edinburgh, and Dublin Philosophical Magazine and Journal of Science **1874**, 218.
[91] R. Ravindran, S. Hassan, G. Williams, A. Jaiswal, *BioEngineering* **2018**, *5*, 93.
[92] S. N. Bose, S. Mukharjee, S. Shrivastava, in *Proc. 4th Jr. Conv. STA, DSTA SISTA*, **1971**, p. 21.
[93] S. Gupta, K. C. Suri, S. K. Bose, *Proc. Annu. Conv. Sugar Technol. Assoc. India* **1980**, *44*, 25.
[94] T. Roberts, J. Dale, J. D. Pritschard, *Polytech. J.* **1857**, *145*, 239.
[95] J. T. Bohlmann, C. Cameselle, M. J. Nunez, J. M. Lema, *Bioprocess Eng.* **1998**, *19*, 337–342.
[96] G. M. Gadd, J. Bahri-Esfahani, Q. Li, Y. J. Rhee, Z. Wei, M. Fomina, X. Liang, *Fungal Biol. Rev.* **2014**, *28*, 36–55.
[97] E. Walaszczyk, E. Gąsiorek, W. Podgórski, *Zesz. Probl. Postepow Nauk Roln.* **2018**, 566, 129–138
[98] M. Cefola, B. Pace, *J. Food Process. Preserv.* **2015**, *39*, 2523–2532.
[99] C. Cameselle, J. T. Bohlmann, M. J. Núñez, J. M. Lema, *Bioprocess Eng.* **1998**, *19*, 247–252.
[100] C. Cameselle, *Bioprocess Eng.* **1998**, *19*, 247–252.
[101] "India Glycols | Products | MEG/DEG/TEG," can be found under https://www.indiaglycols.com/product_groups/monoethylene_glycol.htm, **2021**.
[102] J. C. Van Der Waal, G. J. M. Gruter, E. J. Ras, Avantium Knowledge Centre BV EP3245180A1, **2016**.
[103] P. Levi, T. Vass, H. Mandová, A. Gouy, A. Schröder, *Chemicals (Paris), International Energy Agency, can be found under https://www.iea.org/reports/chemicals* **2020**.
[104] L. A. Pfaltzgraff, J. H. Clark in *Advances in Biorefineries*, Elsevier, **2014**, pp. 3–33.
[105] J. B. Binder, R. T. Raines, *J. Am. Chem. Soc.* **2009**, *131*, 1979–1985.
[106] W. Riemenschneider, M. Tanifuji in *Ullmann's Encyclopedia of Industrial Chemistry*, Wiley-VCH, Weinheim, **2012**, pp. 529–541.
[107] D. F. Kirk, R. E. & Othmer, Oxalic Acid – Kirk-Othmer Encyclopedia of Chemical Technology, **2000**.
[108] T. Yamasaki, M. Eguchi, S. Uchiumi, K. Nishihira, M. Yamashita, H. Itatani, Ube Industries Ltd, US4138587A, **1977**.
[109] K. Nishimura, S. Uchiumi, K. Fujii, K. Nishihira, M. Yamashita, H. Itatani, Ube Industries Ltd, US4229589A, **1978**.
[110] H. Miyazaki, Ya. Shiomi, S. Fujitus, K. Masunaga, H. Yanagisawa, Ube Industries LtdUS4384133, **1982**.
[111] T. Matsuzaki, A. Nakamura, *Catal. Surv. Jpn.* **1997**, *1*, 77–88.
[112] J. Fang, B. Wang, Z. Li, G. Xu, *React. Kinet. Catal. Lett.* **2003**, *80*, 293–301.
[113] T. Yamazaki, M. Eguchi, S. Uchiumi, A. Iwayama, M. Takahashi, M. Kurahashi, Ube Industries Ltd US3994960A, **1975**.
[114] J. Fang, B. Wang, L. Zhenhua, G. Xu, *React. Kinet. Catal. Lett.* **2003**, *80*, 293–301.
[115] Gallently, *Polytech. J.* **1882**, *244*.
[116] S. Verma, B. Kim, H. R. M. Jhong, S. Ma, P. J. A. Kenis, *ChemSusChem* **2016**, *9*, 1972–1979.
[117] M. A. N. Thonemann, *Appl. Energy* **2020**, *263*, 114599.
[118] M. Aresta, A. Dibenedetto, *J. Chem. Soc. Dalton Trans.* **2007**, 2975–2992. 28
[119] K. Armstrong, P. Sanderson, P. Styring in *Fundamentals*, De Gruyter, Berlin, Boston, **2019**, pp. 47–62.
[120] T. Hills, D. Leeson, N. Florin, P. Fennell, *Environ. Sci. Technol.* **2016**, *50*, 368–377.
[121] A. Keys, M. van Hout, B. Daniels, *Decarbonisation Options for the Dutch Steel Industry (Den Haag)* **2019** can be found under: https://www.pbl.nl/en/publications/decarbonisation-options-for-the-dutch-steel-industry
[122] E. Alper, O. Yuksel Orhan, *Petroleum* **2017**, *3*, 109–126.
[123] M. Bui, C. S. Adjiman, A. Bardow, E. J. Anthony, A. Boston, S. Brown, P. S. Fennell, S. Fuss, A. Galindo, L. A. Hackett, J. P. Hallett, H. J. Herzog, G. Jackson, J. Kemper, S. Krevor, et al., *Energy Environ. Sci.* **2018**, *11*, 1062.
[124] R. Bennett, S. Clifford, K. Anderson, G. Puxty in *Energy Procedia*, Elsevier Ltd, **2017**, pp. 1–6.
[125] Y. Wang, L. Zhao, A. Otto, M. Robinius, D. Stolten in *Energy Procedia*, Elsevier Ltd, **2017**, pp. 650–665.
[126] H. Yang, Z. Xu, M. Fan, R. Gupta, R. B. Slimane, A. E. Bland, I. Wright, *J. Environ. Sci.* **2008**, *20*, 14–27.
[127] D. Aaron, C. Tsouris, *Sep. Sci. Technol.* **2005**, *40*, 321–348.
[128] Z. Twardowski, E. Barton Cole, J. J. Kaczur, K. Teamey, K. A. Keets, R. R. Parajuli, A. Bauer, N. Sivansankar, G. Leonard, T. J. Kramer, P. Majsztrik, Y. Zhu, Avantium Knowledge Centre BV US9267212B2, **2016**.
[129] Y. Hori in *Modern Aspects of Electrochemistry*, Springer, New York, NY, **2008**, pp. 89–189.
[130] S. Ikeda, T. Takagi, K. Ito, *Bull. Chem. Soc. Jpn.* **1987**, *60*, 2517–2522.
[131] U. Kaiser, E. Heitz, *Ber. Bunsen-Ges.* **1973**, *77*, 818–823.
[132] J. C. Gressin, D. Michelet, L. Nadjo, J. M. Saveant, *Chem. Informationsdienst* **1979**, *10*, 10.
[133] W. Paik, T. N. Andersen, H. Eyring, *Electrochim. Acta* **1969**, *14*, 1217–1232.
[134] J. L. Roberts, D. T. Sawyer, *J. Electroanal. Chem.* **1965**, *9*, 1–7.
[135] B. Eneau-Innocent, D. Pasquier, F. Ropital, J. M. Léger, K. B. Kokoh, *Appl. Catal. B* **2010**, *98*, 65–71.
[136] E. E. Benson, C. P. Kubiak, A. J. Sathrum, J. M. Smieja, *Chem. Soc. Rev.* **2009**, *38*, 89–99.
[137] C. Amatore, J. M. Saveant, *J. Am. Chem. Soc.* **1981**, *103*, 5021–5023.
[138] L. V. Haynes, D. T. Sawyer, *Anal. Chem.* **1967**, *39*, 332–338.
[139] Y. Oh, H. Vrubel, S. Guidoux, X. Hu, *Chem. Commun.* **2014**, *50*, 3878.
[140] Y. Kushi, H. Nagao, T. Nishioka, K. Isobe, K. Tanaka, *Chem. Lett.* **1994**, *23*, 2175–2178.
[141] K. Ito, S. Ikeda, N. Yamauchi, T. Iida, T. Takagi, *Bull. Chem. Soc. Jpn.* **1985**, *58*, 3027–3028.
[142] A. V. Rudnev, U. E. Zhumaev, A. Kuzume, S. Vesztergom, J. Furrer, P. Broekmann, T. Wandlowski, *Electrochim. Acta* **2016**, *189*, 38–44.
[143] M. C. Figueiredo, I. Ledezma-Yanez, M. T. M. Koper, *ACS Catal.* **2016**, *6*, 2382–2392.
[144] T. C. Berto, L. Zhang, R. J. Hamers, J. F. Berry, *ACS Catal.* **2015**, *5*, 703–707.
[145] S. Kaneco, K. Iiba, K. Ohta, T. Mizuno, A. Saji, *J. Electroanal. Chem.* **1998**, *441*, 215–220.
[146] H. J. Fischer, L. E. Heitz, Dechema Deutsche Gesellschaft fuer Chemisches Apparatewesen eV DE2854487A1, **1978**.
[147] J. Fischer, T. Lehmann, E. Heitz, *J. Appl. Electrochem.* **1981**, *11*, 743–750.
[148] A. R. Paris, A. B. Bocarsly, *ACS Catal.* **2019**, *9*, 2324–2333.
[149] J. Y. Becker, B. Vainas, R. E. Née Levin, L. K. Née Orenstein, *J. Chem. Soc. Chem. Commun.* **1985**, 1471–1472.
[150] Y. Kushi, H. Nagao, T. Nishioka, K. Isobe, K. Tanaka, *J. Chem. Soc. Chem. Commun.* **1995**, *12*, 1223–1224.
[151] W. J. Evans, C. A. Seibel, J. W. Ziller, *Inorg. Chem.* **1998**, *37*, 770–776.
[152] Y. Kushi, H. Nagao, T. Nishioka, K. Isobe, K. Tanaka, *Chem. Lett.* **1994**, *23*, 2175–2178.
[153] R. Angamuthu, P. Byers, M. Lutz, A. L. Spek, E. Bouwman, *Science* **2010**, *327*, 313–315.
[154] U. R. Pokharel, F. R. Fronczek, A. W. Maverick, *Nat. Commun.* **2014**, *5*, 5883.
[155] F. Khamespanah, M. Marx, D. B. Crochet, U. R. Pokharel, F. R. Fronczek, A. W. Maverick, M. Beller, *Nat. Commun.* **2021**, *12*, 1–4.
[156] R. Senthil Kumar, S. Senthil Kumar, M. Anbu Kulandainathan, *Electrochem. Commun.* **2012**, *25*, 70–73.
[157] L. Pastero, N. Curetti, M. A. Ortenzi, M. Schiavoni, E. Destefanis, A. Pavese, *Sci. Total Environ.* **2019**, *666*, 1232–1244.
[158] T. Matsui, Y. Kitagawa, M. Okumura, Y. Shigeta, *J. Phys. Chem. A* **2015**, *119*, 369–376.
[159] V. Elste, K. Peng, A. Kleefeldt, G. Litta, J. Medlock, G. Pappenberger, B. Oster, U. Fechtel, in *Ullmann's Encyclopedia of Industrial Chemistry*, Wiley-VCH, Weinheim, **2020**, pp. 1–21.
[160] G. Laber in *Ullmanns Enzyklopädie Der Technischen Chemie*, Wiley-VCH Verlag, Weinheim, **1962**, pp. 51–55.
[161] D. M. Fenton, P. J. Steinwand, *J. Org. Chem.* **1974**, *39*, 701–704.
[162] J. Bierhals in *Ullmann's Encyclopedia of Industrial Chemistry*, Wiley-VCH, Weinheim, **2012**, pp. 679–691.
[163] A. Haynes, P. M. Maitlis, G. E. Morris, G. J. Sunley, H. Adams, P. W. Badger, C. M. Bowers, D. B. Cook, P. I. P. Elliott, T. Ghaffar, H. Green, T. R. Griffin, M. Payne, J. M. Pearson, M. J. Taylor, P. W. Vickers, R. J. Watt, *J. Am. Chem. Soc.* **2004**, *126*, 2847–2861.

[164] G. Centi, E. A. Quadrelli, S. Perathoner, *Energy Environ. Sci.* **2013**, *6*, 1711–1731.
[165] Y. A. Daza, J. N. Kuhn, *RSC Adv.* **2016**, *6*, 49675–49691.
[166] W. Wang, S. Wang, X. Ma, J. Gong, *Chem. Soc. Rev.* **2011**, *40*, 3703–3727.
[167] T. Zheng, K. Jiang, H. Wang, *Adv. Mater.* **2018**, *30*, 1802066.
[168] A. R. C. Morais, A. M. da Costa Lopes, R. Bogel-Łukasik, *Chem. Rev.* **2015**, *115*, 3–27.
[169] P. Lahijani, Z. A. Zainal, M. Mohammadi, A. R. Mohamed, *Renewable Sustainable Energy Rev.* **2015**, *41*, 615–632.
[170] A. Aho, N. Kumar, K. Eränen, T. Salmi, M. Hupa, D. Y. Murzin, *Process Saf. Environ. Prot.* **2007**, *85*, 473–480.
[171] Y. H. Chan, K. V. Dang, S. Yusup, M. T. Lim, A. M. Zain, Y. Uemura, *J. Energy Inst.* **2014**, *87*, 227–234.
[172] M. K. Lam, A. C. M. Loy, S. Yusup, K. T. Lee in *Biohydrogen*, Elsevier, **2019**, pp. 219–245.
[173] C. Bosch, W. Wild, BASF SE US1115776A, **1913**.
[174] X. Xiaoding, J. A. Moulijn, *Energy Fuels* **1996**, *10*, 305–325.
[175] S. Nitopi, E. Bertheussen, S. B. Scott, X. Liu, A. K. Engstfeld, S. Horch, B. Seger, I. E. L. Stephens, K. Chan, C. Hahn, J. K. Nørskov, T. F. Jaramillo, I. Chorkendorff, *Chem. Rev.* **2019**, *119*, 7610–7672.
[176] C. S. Chen, J. H. Lin, J. H. You, C. R. Chen, *J. Am. Chem. Soc.* **2006**, *128*, 15950–15951.
[177] G. C. Chinchen, M. S. Spencer, K. C. Waugh, D. A. Whan, *J. Chem. Soc. Faraday Trans. 1* **1987**, 2193–2212.
[178] K. Klier, C. W. Young, J. G. Nunan, *Ind. Eng. Chem. Fundam.* **1986**, *25*, 36–42.
[179] D. S. Newsome, *Catal. Rev.* **1980**, *21*, 275–318.
[180] A. J. Martín, G. O. Larrazábal, J. Pérez-Ramírez, *Green Chem.* **2015**, *17*, 5114–5130.
[181] F. Bienen, D. Kopljar, A. Löwe, P. Aßmann, M. Stoll, P. Rößner, N. Wagner, A. Friedrich, E. Klemm, *Chem. Ing. Tech.* **2019**, *91*, 872–882.
[182] D. U. Nielsen, X. M. Hu, K. Daasbjerg, T. Skrydstrup, *Nat. Catal.* **2018**, *1*, 244–254.
[183] S. Hernández, M. Amin Farkhondehfal, F. Sastre, M. Makkee, G. Saracco, N. Russo, *Green Chem.* **2017**, *19*, 2326–2346.
[184] C. Chen, J. F. Khosrowabadi Kotyk, S. W. Sheehan, *Chem* **2018**, *4*, 2571–2586.
[185] S. Ikeda, T. Takagi, K. Ito, *Bull. Chem. Soc. Jpn.* **1987**, *60*, 2517–2522.
[186] J. Durst, A. Rudnev, A. Dutta, Y. Fu, J. Herranz, V. Kaliginedi, A. Kuzume, A. A. Permyakova, Y. Paratcha, P. Broekmann, T. J. Schmidt, *Chimia* **2015**, *69*, 769–776.
[187] C. Oloman, H. Li, *ChemSusChem* **2008**, *1*, 385–391.
[188] S. Das, W. M. A. Wan Daud, *RSC Adv.* **2014**, *4*, 20856.
[189] P. R. Yaashikaa, P. Senthil Kumar, S. J. Varjani, A. Saravanan, *J. $CO_2$ Util.* **2019**, *33*, 131–147.
[190] W. C. Chueh, C. Falter, M. Abbott, D. Scipio, P. Furler, S. M. Haile, A. Steinfeld, *Science* **2010**, *330*, 1797–1801.
[191] P. Furler, J. Scheffe, M. Gorbar, L. Moes, U. Vogt, A. Steinfeld, *Energy Fuels* **2012**, *26*, 7051–7059.
[192] A. H. McDaniel, E. C. Miller, D. Arifin, A. Ambrosini, E. N. Coker, R. O'Hayre, W. C. Chueh, J. Tong, *Energy Environ. Sci.* **2013**, *6*, 2424.
[193] J. E. Miller, M. D. Allendorf, R. B. Diver, L. R. Evans, N. P. Siegel, J. N. Stuecker, *J. Mater. Sci.* **2008**, *43*, 4714–4728.
[194] N. B. Jakobsson, C. F. Pedersen, J. B. Hansen, Haldor Topsoe AS US10494728, **2019**.
[195] S. Uchiumi, K. Ataka, T. Matsuzaki, *J. Organomet. Chem.* **1999**, *576*, 279–289.
[196] X.-Z. Jiang, *Platinum Met. Rev.* **1990**, *34*, 178–180.
[197] R. Noyori, Y. G. K. Kyōkai, Tokyo Kagaku Dozin, Tokyo; **1992**, pp. 500–501.
[198] G. Cohn in *Ullman's Encyclopedia of Industrial Chemistry*, Wiley-VCH, Weinheim, **1929**, pp. 426–429.
[199] O. Horn in *Ullmanns Enzyklopädie Der Technischen Chemie*, Wiley-VCH, Weinheim, **1953**, pp. 73–78.
[200] J. Weise, F. Rieche, A. Barth, Rudolph Koepp & Co Koepp & Co R US820159 A, **1906**.
[201] A. Berthelot, *Nuovo Cimento Ser. 3* **1856**, *61*, 463.
[202] J. Hietala, A. Vuori, P. Johnsson, I. I. Pollari, W. Reutemann, H. Kieczka in *Ullmann's Encyclopedia of Industrial Chemistry*, Wiley-VCH, Weinheim, **2016**, pp. 335–340.
[203] L. G. Lundsted, *J. Am. Chem. Soc.* **1949**, *71*, 323–324.
[204] S. Teir, S. Eloneva, R. Zevenhoven in *ECOS 2005 – Proc. 18th Int. Conf. Effic. Cost*, Optim. Simulation, Environ. Impact Energy Syst., **2005**, pp. 749–756.
[205] Y. Yu, B. Chen, W. Qi, X. Li, Y. Shin, C. Lei, J. Liu, *Microporous Mesoporous Mater.* **2012**, *153*, 166–170.
[206] G. Bredig, S. R. Carter, *Ber. Dtsch. Chem. Ges.* **1914**, *47*, 541–545.
[207] H. Wiener, J. Blum, H. Feilchenfeld, Y. Sasson, N. Zalmanov, *J. Catal.* **1988**, *110*, 184–190.
[208] S. P. Kamble, R. G. Kalshetti, V. Vaithiyanathan, A. Sudalai, Council Of Scientific & Industrial Research; WO2016024293 A1, **2016**.
[209] T. Zhao, X. Hu, Y. Wu, Z. Zhang, *Angew. Chem. Int. Ed.* **2019**, *58*, 722–726; *Angew. Chem.* **2019**, *131*, 732–736.
[210] A. Kumar, S. Semwal, J. Choudhury, *ACS Catal.* **2019**, *9*, 2164–2168.
[211] T. Cheng, H. Xiao, W. A. Goddard, *J. Am. Chem. Soc.* **2016**, *138*, 13802–13805.
[212] A. S. Agarwal, Y. Zhai, D. Hill, N. Sridhar, *ChemSusChem* **2011**, *4*, 1301–1310.
[213] S. Trasatti, *J. Electroanal. Chem. Interfacial Electrochem.* **1972**, *39*, 163–184.
[214] W. Ma, S. Xie, X.-G. Zhang, F. Sun, J. Kang, Z. Jiang, Q. Zhang, D.-Y. Wu, Y. Wang, *Nat. Commun.* **2019**, *10*, 892.
[215] D. Pavesi, F. S. M. Ali, D. Anastasiadou, T. Kallio, M. Figueiredo, G. J. M. Gruter, M. T. M. Koper, K. J. P. Schouten, *Catal. Sci. Technol.* **2020**, *10*, 4264–4270.
[216] D. Pavesi, R. C. J. Van De Poll, J. L. Krasovic, M. Figueiredo, G. J. M. Gruter, M. T. M. Koper, K. J. P. Schouten, *ACS Sustainable Chem. Eng.* **2020**, *8*, 15603–15610.
[217] Y. Hori, K. Kikuchi, S. Suzuki, *Chem. Lett.* **1985**, *14*, 1695–1698.
[218] R. Zhang, W. Lv, L. Lei, *Appl. Surf. Sci.* **2015**, *356*, 24–29.
[219] P. Quaino, F. Juarez, E. Santos, W. Schmickler, *Beilstein J. Nanotechnol.* **2014**, *5*, 846–854.
[220] J. Wu, Y. Huang, W. Ye, Y. Li, *Adv. Sci.* **2017**, *4*, 170–194.
[221] Z. Yang, F. E. Oropeza, K. H. L. Zhang, *APL Mater.* **2020**, *8*, 60901.
[222] H. Li, C. Oloman, *J. Appl. Electrochem.* **2007**, *37*, 1107–1117.
[223] N. I. Hammer, S. Sutton, J. Delcamp, J. D. Graham, in *Handb. Clim. Chang. Mitig. Adapt.*, Springer International Publishing, Cham, **2017**, pp. 2709–2756.
[224] R. R. Rodrigues, C. M. Boudreaux, E. T. Papish, J. H. Delcamp, *ACS Appl. Mater. Interfaces* **2019**, *2*, 37–46.
[225] M. Borges Ordoño, A. Urakawa, *J. Phys. Chem. C* **2019**, *123*, 4140–4147.
[226] Q. Xiang, B. Cheng, J. Yu, *Angew. Chem. Int. Ed.* **2015**, *54*, 11350–11366; *Angew. Chem.* **2015**, *127*, 11508–11524.
[227] N. Sutin, C. Creutz, E. Fujita, *Comments Inorg. Chem.* **1997**, *19*, 67–92.
[228] H. Ishida, T. Terada, K. Tanaka, T. Tanaka, *Inorg. Chem.* **1990**, *29*, 905–911.
[229] G. Sahara, O. Ishitani, *Inorg. Chem.* **2015**, *54*, 5096–5104.
[230] C. M. Boudreaux, N. P. Liyanage, H. Shirley, S. Siek, D. L. Gerlach, F. Qu, J. H. Delcamp, E. T. Papish, *Chem. Commun.* **2017**, *53*, 11217–11220.
[231] R. N. Sampaio, D. C. Grills, D. E. Polyansky, D. J. Szalda, E. Fujita, *J. Am. Chem. Soc.* **2020**, *142*, 2413–2428.
[232] Y. Hameed, P. Berro, B. Gabidullin, D. Richeson, *Chem. Commun.* **2019**, *55*, 11041–11044.
[233] Y. Hameed, G. K. Rao, J. S. Ovens, B. Gabidullin, D. Richeson, *ChemSusChem* **2019**, *12*, 3453–3457.
[234] H. Ishida, A. Sakaba, *Faraday Discuss.* **2017**, *198*, 263–277.
[235] C.-Y. Zhu, Y.-Q. Zhang, R.-Z. Liao, W. Xia, J.-C. Hu, J. Wu, H. Liu, F. Wang, *Dalton Trans.* **2018**, *47*, 13142–13150.
[236] Q. Zhai, S. Xie, W. Fan, Q. Zhang, Y. Wang, W. Deng, Y. Wang, *Angew. Chem. Int. Ed.* **2013**, *52*, 5776–5779; *Angew. Chem.* **2013**, *125*, 5888–5891.
[237] H. Zhou, J. Guo, P. Li, T. Fan, D. Zhang, J. Ye, *Sci. Rep.* **2013**, *3*, 1667.
[238] C. Mourato, M. Martins, S. M. da Silva, I. A. C. Pereira, *Bioresour. Technol.* **2017**, *235*, 149–156.
[239] Y. Amao, *J. $CO_2$ Util.* **2018**, *26*, 623–641.
[240] M. Yuan, S. Sahin, R. Cai, S. Abdellaoui, D. P. Hickey, S. D. Minteer, R. D. Milton, *Angew. Chem. Int. Ed.* **2018**, *57*, 6582–6586.
[241] D. Niks, R. Hille in *Methods in Enzymology*, Academic Press Inc., **2018**, pp. 277–295.
[242] D. Alagöz, A. Çelik, D. Yildirim, S. S. Tükel, B. Binay, *J. Mol. Catal. B* **2016**, *130*, 40–47.
[243] Y. Wang, Z. Zhao, M. Li, Y. Chen, W. Liu, *J. Membr. Sci.* **2016**, *514*, 44–52.
[244] D. Yildirim, D. Alagöz, A. Toprak, S. Tükel, R. Fernandez-Lafuente, *Process Biochem.* **2019**, *85*, 97–105.
[245] R. Wu, C. Ma, Z. Zhu, *Curr. Opin. Electrochem.* **2020**, *19*, 1–7.
[246] M. Lienemann, J. S. Deutzmann, R. D. Milton, M. Sahin, A. M. Spormann, *Bioresour. Technol.* **2018**, *254*, 278–283.

[247] F. Gu, Y. Wang, Z. Meng, W. Liu, L. Qiu, *Catal. Commun.* **2020**, *136*, 105903.
[248] R. Barin, D. Biria, S. Rashid-Nadimi, M. A. Asadollahi, *Chem. Eng. Process. Process Intensif.* **2019**, *140*, 78–84.
[249] V. Merz, W. Weith, *Ber. Dtsch. Chem. Ges.* **1882**, *15*, 1507–1513.
[250] J. L. Gay-Lussac, *Polytech. J.* **1831**, *41*, 222–223.
[251] M. Goldschmidt, US659733A, **1900**.
[252] J. Wimmer, Consortium fuer Elektrochemische Industrie GmbH DE588159, **1933**.
[253] H. Hoff, Koepp & Co R Chem Fab AG FR759216, **1934**.
[254] E. Hene, Rudolph Koepp & Co Chem Fabrik AG US2004867, **1935**.
[255] M. Enderli, Rudolph Koepp & Co Chem Fabrik AG US2002342, **1935**.
[256] M. Enderli, A. Schrodt, Rudolph Koepp & Co Chem Fabrik AG US2033097, **1936**.
[257] A. Wiens, US714347, **1902**.
[258] D. Strauss, Novartis AG US1038985, **1912**.
[259] E. Mewburn, Oldbury Electro Chemical Co GB160747, **1922**.
[260] H. W. Paulus, Royal baking powder Co US1445162, **1923**.
[261] H. W. Paulus, Royal baking powder Co US1445163, **1923**.
[262] W. Wallace, Oldbury Electro Chemical Co US1506872, **1924**.
[263] H. Oehme, Chem Fabrik Kalk GmbH DE414376, **1925**.
[264] O. P. C. Bredt, Trojan Powder Co US1622991, **1927**.
[265] L. K. Freidlin, *Sci. Rep. (Moscow Univ.)* **1936**, 152–156.;
[266] L. K. Freidlin, A. A. Balandin, A. I. Lebedeva, *Russ. Chem. Bull. (Izvestiya Akad. Nauk SSSR)* **1941**, *2*, 255–262.
[267] A. A. Balandin, L. K. Freidlin, *Zh. Obshch. Khim.* **1935**, *6*, 868–872.
[268] L. K. Freidlin, *Zh. Prikl. Khim.* **1938**, *11*, 975–980.
[269] L. K. Freidlin, *Zh. Obshch. Khim.* **1937**, *7*, 1675–1683.
[270] L. K. Freidlin, *Promyshlennost Org. Khimii* **1937**, *3*, 681–686.;
[271] L. K. Freidlin, *Trans. All-Union Acad. Food Ind. named after Stalin* **1939**, 145–157. 10
[272] L. K. Freidlin, A. A. Balandin, A. I. Lebedeva, *Russ. Chem. Bull. (Izvestiya Akad. Nauk SSSR)* **1941**, *2*, 247–256.
[273] L. K. Freidlin, *Zh. Prikl. Khim.* **1937**, *10*, 1086–1094.
[274] L. K. Freidlin, A. A. Balandin, A. I. Lebedeva, *Russ. Chem. Bull. (Izvestiya Akad. Nauk SSSR)* **1941**, *2*, 268–274.
[275] A. A. Balandin, L. K. Freidlin, D. N. Vaskevich, *Sci. Repts. Moscow State Univ.* **1936**, *6*, 321–345.
[276] L. K. Freidlin, A. A. Balandin, A. I. Lebedeva, *Russ. Chem. Bull. (Izvestiya Akad. Nauk SSSR)* **1941**, *2*, 261–267.
[277] L. K. Freidlin, A. A. Balandin, A. I. Lebedeva, Bull. acad. sci. U. R. S. S., Classe sci. math. nat., Ser. chim. **1940**, *6*, 955–962.
[278] L. K. Freidlin, A. A. Balandin, A. I. Lebedeva, *Russ. Chem. Bull. (Izvestiya Akad. Nauk SSSR)* **1941**, *2*, 275–288.
[279] A. Górski, A. Kraśnicka, *J. Therm. Anal.* **1987**, *32*, 1243–1251.
[280] A. Górski, A. D. Kraśnicka, *J. Therm. Anal.* **1987**, *32*, 1229–1241.
[281] A. Górski, A. D. Kraśnicka, *J. Therm. Anal.* **1987**, *32*, 1895–1904.
[282] A. Górski, A. D. Kraśnicka, *J. Therm. Anal.* **1987**, *32*, 1345–1354.
[283] S. Shishido, Y. Masuda, *Nippon Kagaku Kaishi* **1976**, *5*, 325–1675.
[284] S. Shishido, Y. Masuda, *Nippon Kagaku Kaishi* **1973**, 185–188. 1
[285] E. Schuler, A. Perez de Alba Ortiz, B. Ensing, N. R. Shiju, G.-J. M. Gruter, *ACS Catal.*, unpublished results.
[286] T. Meisel, Z. Halmos, K. Seybold, E. Pungor, *J. Therm. Anal.* **1975**, *7*, 73–80.
[287] W. C. Butterman, W. E. Brooks, R. G. J. Reese, *U. S. Geol. Surv.* **2004**, 1–10.
[288] L. K. Freidlin, A. I. Lebedeva, *Zhurnal Prikl. Khimii (Sankt-Peterburg, Russ. Fed.* **1937**, *10*, 1086–1094 (in French 1094).
[289] S. Takagi, *Nippon Kagaku Kaishi* **1939**, *60*, 625–631.
[290] E. Schuler, M. Stoop, N. R. Shiju, G.-J. M. Gruter, *ACS Sustainable Chem. Eng.* **2021**, unpublished results.
[291] N. N. Greenwood, A. B. T. Earnshaw in *Chemistry of the Elements*, Elsevier, Oxford, **1997**, pp. 68–106.
[292] R. N. Trubey, *Altern. Ther. Health Med.* **2004**, *11*, 19.
[293] K. Hartman, I. C. Hisatsune, *J. Phys. Chem.* **1966**, *583*, 1281–1287.
[294] D. W. Ovenall, D. H. Whiffen, *Mol. Phys.* **1961**, *4*, 135–144.
[295] A. Paparo, J. Okuda, *J. Organomet. Chem.* **2018**, *869*, 270–274.
[296] A. Li, Z. Li, CN1166482A, **1997**.
[297] A. Li, Y. Li, Taiyuan University of Technology CN101823950A, **2010**.
[298] A. Li, Y. Li, Z. Zhao, A. Zhang, Z. Li, Taiyuan University of Technology CN1903821B, **2012**.
[299] Z. Xu, X. Cheng, W. Xia, Luotian Fuyang Fertilizer CO LtdCN102391099A, **2012**.
[300] H. Jiang, D. Li, Z. Jiang, D. Wang, Z. Ban, B. Zhang, Tianjin Tianyi synthesis engineering carbon Co Ltd CN102659556A, **2012**.
[301] J. H. H. Meurs, Shell Internationale Research Maatschappij B.V., Shell Oil Company WO2016/124646A1, **2016**.
[302] Q. Guo, Ningxia Hainachuan Chemical Technology Co Ltd CN107216248A, **2017**.
[303] X. Yu, CN1502599A, **2004**.
[304] K. Xie, University of Electronic Science and Technology of China CN1727322A, **2006**.
[305] A. Li, Y. Li, Taiyuan University of Technology CN1927805A, **2007**.
[306] Q. Ma, A. Li, Y. Li, Taiyuan University of Technology CN100999462A, **2007**.
[307] A. Li, C. Liu, Q. Li, Taiyuan University of TechnologyCN101077855A, **2007**.
[308] Z. Cao, Y. Cao, Hubei Ze Mao Chemical Co., Ltd. CN201343509Y, **2009**.
[309] W. Wesner, Knoch, Kern & CO. KGWO2009/117753A1, **2009**.
[310] Z. Cao, Y. Cao, Hubei Ze Mao Chemical Co., Ltd. CN101462943A, **2009**.
[311] C. Huang, T. Xu, Y. Zhang, Y. Xue, G. Chen, *J. Membr. Sci.* **2007**, *288*, 1–12.
[312] Z. Yazicigil, *Desalination* **2007**, *212*, 70–78.
[313] K. Scott, *Renewable Sustainable Energy Rev.* **2018**, *81*, 1406–1426.
[314] S. Koter, *Recent Pat. Eng.* **2011**, *4*, 141–160.
[315] H. Strathmann in *Membrane Science & Technoly*, Elsevier, Amsterdam, **2004**, pp. 89–146.
[316] S. Chabi, A. G. Wright, S. Holdcroft, M. S. Freund, *ACS Appl. Mater. Interfaces* **2017**, *9*, 26749–26755.
[317] S. Novalic, T. Kongbangkerd, K. D. Kulbe, *J. Membr. Sci.* **2000**, *166*, 99–104.
[318] J. S. J. Ferrer, S. Laborie, G. Durand, M. Rakib, *J. Membr. Sci.* **2006**, *280*, 509–516.
[319] G. S. Trivedi, B. G. Shah, S. K. Adhikary, V. K. Indusekhar, R. Rangarajan, *React. Funct. Polym.* **1997**, *32*, 209–215.
[320] H. Li, R. Mustacchi, C. J. Knowles, W. Skibar, G. Sunderland, I. Dalrymple, S. A. Jackman, *Tetrahedron* **2004**, *60*, 655–661.
[321] K. Ghyselbrecht, A. Silva, B. Van der Bruggen, K. Boussu, B. Meesschaert, L. Pinoy, *J. Environ. Manage.* **2014**, *140*, 69–75.
[322] M. Herrero-Gonzalez, P. Diaz-Guridi, A. Dominguez-Ramos, A. Irabien, R. Ibañez, *Sep. Purif. Technol.* **2020**, *242*, 116785.
[323] E. Jones, M. Qadir, M. T. H. van Vliet, V. Smakhtin, S. Mu Kang, *Sci. Total Environ.* **2019**, *657*, 1343–1356.
[324] K. Ghyselbrecht, B. Sansen, A. Monballiu, Z. L. Ye, L. Pinoy, B. Meesschaert, *Sep. Purif. Technol.* **2019**, *221*, 12–22.
[325] Y. Song, Z. Zhao, *Sep. Purif. Technol.* **2018**, *206*, 335–342.
[326] J. Morillo, J. Usero, D. Rosado, H. El Bakouri, A. Riaza, F. J. Bernaola, *Desalination* **2014**, *336*, 32–49.
[327] E. Sanada, T. Yonemitsu, T. Isshika, A. Suzuki, Mitsubishi Edogawa Kagaku KK US3691232, **1969**.
[328] E. Yonemitsu, T. Isshiki, T. Suzuki, Y. Yashima, Mitsubishi Edogawa Kagaku KK DE2011998A, US3678107, **1972**.
[329] B. Wieland, J. P. Lancaster, C. S. Hoaglund, P. Holota, W. J. Tornquist, *Langmuir* **1996**, *12*, 2594–2601.
[330] H. Wang, Z. Jusys, R. J. Behm, *J. Electroanal. Chem.* **2006**, *595*, 23–36.
[331] T. Takeguchi, H. Arikawa, M. Yamauchi, R. Abe in *ECS Trans.* **2011**, pp. 1755–1759.
[332] K.-R. Hwang, W. Jeon, S. Y. Lee, M.-S. Kim, Y.-K. Park, *Chem. Eng. J.* **2020**, *390*, 124–636.
[333] S. Kandasamy, S. P. Samudrala, S. Bhattacharya, *Catal. Sci. Technol.* **2019**, *9*, 567–577.
[334] S. Rebsdat, D. Mayer in *Ullmann's Encyclopedia of Industrial Chemistry*, Wiley-VCH, Weinheim, **2000**, pp. 547–572.
[335] A. Alias, R. Awang, A Review on the Production of Glycol from Glycerol, **2010**.
[336] H. Kobayashi, A. Fukuoka in *New and Future Developments in Catalysis*, Elsevier, **2013**, pp. 29–52.
[337] H. Yue, Y. Zhao, X. Ma, J. Gong, *Chem. Soc. Rev.* **2012**, *41*, 4218–4244.
[338] K. Zhang, S. Wu, H. Yang, H. Yin, G. Li, *RSC Adv.* **2016**, *6*, 77499–77506.
[339] K. Dong, S. Elangovan, R. Sang, A. Spannenberg, R. Jackstell, K. Junge, Y. Li, M. Beller, *Nat. Commun.* **2016**, *7*, 1–7.
[340] E. M. Belgsir, E. Bouhier, H. Essis Yei, K. B. Kokoh, B. Beden, H. Huser, J.-M. Leger, C. Lamy, *Electrochim. Acta* **1991**, *36*, 1157–1164.
[341] G. Horányi, V. E. Kazarinov, Y. B. Vassiliev, V. N. Andreev, *J. Electroanal. Chem. Interfacial Electrochem.* **1983**, *147*, 263–278.
[342] A. Dailey, J. Shin, C. Korzeniewski, *Electrochim. Acta* **1998**, *44*, 1147–1152.
[343] P. Eisele, R. Killpack in *Ullmann's Encyclopedia of Industrial Chemistry*, Wiley-VCH, Weinheim, **2011**, pp. 769–792.

[344] Y. Gao, L. Neal, D. Ding, W. Wu, C. Baroi, A. M. Gaffney, F. Li, *ACS Catal.* **2019**, *9*, 8592–8621.
[345] H. Zimmermann in *Ullmann's Encyclopedia of Industrial Chemistry*, Wiley-VCH, Weinheim, Germany, **2013**, pp. 1–16.
[346] D. F. Rodríguez-Vallejo, G. Guillén-Gosálbez, B. Chachuat, *ACS Sustainable Chem. Eng.* **2020**, *8*, 3072–3081.
[347] M. Kelly, *Propylene Process Summary* **2016**, 6-17.
[348] H. M. Torres Galvis, K. P. De Jong, *ACS Catal.* **2013**, *3*, 2130–2149.
[349] T. Ren, M. Patel, K. Blok, *Energy* **2006**, *31*, 425–451.
[350] F. Xu, S. G. Bell, J. Lednik, A. Insley, Z. Rao, L.-L. Wong, *Angew. Chem. Int. Ed.* **2005**, *44*, 4029–4032; *Angew. Chem.* **2005**, *117*, 4097–4100.
[351] I. Takahara, M. Saito, M. Inaba, K. Murata, *Catal. Lett.* **2005**, *105*, 249–252.
[352] A. Mohsenzadeh, A. Zamani, M. J. Taherzadeh, *Chem. Bio. Eng. Rev.* **2017**, *4*, 75–91.
[353] Nexant. Inc., *PERP Report "Green Propylene" (London)* **2009**.
[354] Nexant. Inc., *PERP Report "Propylene" (London)* **2008**.
[355] J. Gao, C. Jia, B. Liu, *Catal. Sci. Technol.* **2017**, *7*, 5602–5607.
[356] P. G. Machado, A. Walter, M. Cunha, *Biofuels Bioprod. Biorefin.* **2016**, *10*, 623–633.
[357] J. Caner, Z. Liu, Y. Takada, A. Kudo, H. Naka, S. Saito, *Catal. Sci. Technol.* **2014**, *4*, 4093–4098.
[358] Alex Tullo, *C & EN Glob. Enterp.* **2021**, *99*, 14–14.
[359] N. S. Shamsul, S. K. Kamarudin, N. A. Rahman, N. T. Kofli, *Renewable Sustainable Energy Rev.* **2014**, *33*, 578–588.
[360] H. Nakagawa, T. Harada, T. Ichinose, K. Takeno, S. Matsumoto, M. Kobayashi, M. Sakai, *Jpn. Agric. Res. Q.* **2007**, *41*, 173–180.
[361] R. Sindhu, P. Binod, A. Pandey, S. Ankaram, Y. Duan, M. K. Awasthi in *Current Developments in Biotechnology and Bioengineering*, Elsevier, **2019**, pp. 79–92.
[362] V. Zacharopoulou, A. Lemonidou, *Catalysts* **2017**, *8*, 2.
[363] E. E. Gilbert, E. J. Carlson, US3081345A, **1960**.
[364] J. P. Agrawal, R. D. Hodgson in *Organic Chemistry of Explosives*, Wiley, Chichester, **2006**, pp. 1–7.
[365] J. M. Duroux, L. M. E. Pichon, US3549696A, **1966**.
[366] A. Charamel, J. M. Duroux, S. Siquet, J. Descroix, *A. Charamel*, US3692830A, **1970**.
[367] W. Riemenschneider, M. Tanifuji, Wiley-VCH, **2012**, *25*, 529–541.
[368] J. Valentine, J. Clifton-Brown, A. Hastings, P. Robson, G. Allison, P. Smith, *GCB Bioenergy* **2012**, *4*, 1–19.
[369] A. J. Haughton, A. J. Bond, A. A. Lovett, T. Dockerty, G. Sünnenberg, S. J. Clark, D. A. Bohan, R. B. Sage, M. D. Mallott, V. E. Mallott, M. D. Cunningham, A. B. Riche, I. F. Shield, J. W. Finch, M. M. Turner, A. Karp, *J. Appl. Ecol.* **2009**, *46*, 315–322.
[370] B. Holmatov, A. Y. Hoekstra, M. S. Krol, *Renewable Sustainable Energy Rev.* **2019**, *111*, 224–235.
[371] A. Y. Hoekstra, T. O. Wiedmann, *Science* **2014**, *344*, 1114–1117.
[372] R. Murphy, J. Woods, M. Black, M. McManus, *Food Policy* **2011**, *36*, S52–S61.
[373] J. Kemper, *Int. J. Greenhouse Gas Control* **2015**, *40*, 401–430.
[374] I. F. Bitterfeld, *Inbetriebnahme Der Neuen Oxalsäure Anlage*, Landesarchiv Sachsen-Anhalt, Abteilung Merseburg, **1932**.
[375] D. Hackenholz, Die Elektrochemischen Werke in Bitterfeld, 1914–1945: Ein Standort Der IG-Farbenindustrie AG, LIT Verlag, **2004**.
[376] J. W. Nyren, *Polytech. J.* **1841**, *81*, 124–125.
[377] E. Sarka, Z. Bubnik, A. Hinkova, J. Gebler, P. Kadlec, *Procedia Eng.* **2012**, *42*, 1219–1228.
[378] R. Ravindran, S. Hassan, G. Williams, A. Jaiswal, *BioEngineering* **2018**, *5*, 93.
[379] D. F. Kirk, R. E. & Othmer, Interscience Publishers, **1967**, pp. 366–372.
[380] G. H. F. E. Watson, W. E. Watson, G. H. Fuchs, US3536754A, **1968**.
[381] M. J. Brooks, US2322915A, **1943**.
[382] W.Thorn, Preparation of Oxalic Acid from Sawdust, Bran and Lignose 218, **1874**.
[383] L. Possoz, *Polytech. J.* **1858**, *150*.
[384] P. Anastas, N. Eghbali, *Chem. Soc. Rev.* **2010**, *39*, 301–312.

Manuscript received: June 18, 2021
Revised manuscript received: July 28, 2021
Accepted manuscript online: July 29, 2021
Version of record online: August 19, 2021